

**Figure 1.** (a) Frontier molecular orbital interaction in normal-electron-demand DA reaction and DA activation by an LA and encapsulated ion. (b) Differences in electronic and steric factors between Li<sup>+</sup>@C<sub>60</sub> and empty C<sub>60</sub> influenced the DA reaction rate. EWG, electron-withdrawing group; EDG, electron-donating group.

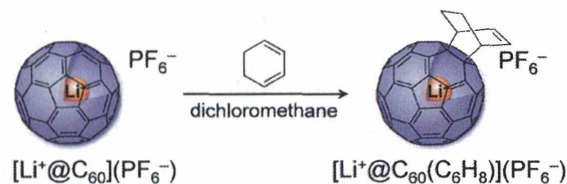
Li<sup>+</sup>. This result stands in contrast to the findings on neutral endohedral fullerenes such as He@C<sub>60</sub>, H<sub>2</sub>@C<sub>60</sub>, and H<sub>2</sub>@C<sub>70</sub>, which are not known to enhance reactivity of the DA reactions.<sup>9</sup> However, because the DA reaction of Li<sup>+</sup>@C<sub>60</sub> with cyclopentadiene was extremely fast, we were unable to conduct a quantitative analysis of the kinetics.<sup>8</sup> This can be seen by comparing the second-order rate constants (*k*<sub>2</sub>) for the DA reaction of empty C<sub>60</sub> with cyclopentadiene (1.70 × 10<sup>-1</sup> M<sup>-1</sup> s<sup>-1</sup>) and 1,3-cyclohexadiene (6.71 × 10<sup>-5</sup> M<sup>-1</sup> s<sup>-1</sup>) in toluene at 30 °C, as shown in Supporting Information Table S2.

In this study, we kinetically and computationally investigated the DA reaction of Li<sup>+</sup>@C<sub>60</sub> with 1,3-cyclohexadiene (C<sub>6</sub>H<sub>8</sub>) and precisely determined the activation energy *E*<sub>a</sub> and other kinetic parameters. Together with the reported DA reactivity of other endohedral metallofullerenes,<sup>10</sup> our observed kinetics data on the DA reaction of Li<sup>+</sup>@C<sub>60</sub> will provide basic knowledge that should be useful for the chemical functionalization of endohedral fullerenes and, more generally, for the understanding of DA chemistry. Our results suggest that Li<sup>+</sup>@C<sub>60</sub> will be useful as a core unit of functionalized nanomaterials in organic electronics and medicinal chemistry.<sup>11</sup>

## RESULTS AND DISCUSSION

**Synthesis and Characterization of the DA Adduct of Li<sup>+</sup>@C<sub>60</sub> and 1,3-Cyclohexadiene.** To study the kinetics of the DA reaction, we chose 1,3-cyclohexadiene (C<sub>6</sub>H<sub>8</sub>) because of its simple structure and suitable reactivity toward both C<sub>60</sub> and Li<sup>+</sup>@C<sub>60</sub>. In our experiments, the second-order rate constants for DA reactions of empty C<sub>60</sub> with various 1,3-dienes at 303 K were distributed over a wide range: *k*<sub>2</sub> = 1.8 × 10<sup>-5</sup> to 1.7 × 10<sup>-1</sup> M<sup>-1</sup> s<sup>-1</sup> (Supporting Information Table S2). All reactions were carried out in the dark (Scheme 1). Reaction progress was monitored by an HPLC technique using an electrolyte-containing mobile phase,<sup>8,11</sup> and the monoadduct product was isolated by preparative HPLC. The product [Li<sup>+</sup>@C<sub>60</sub>(C<sub>6</sub>H<sub>8</sub>)](PF<sub>6</sub><sup>-</sup>) was very stable in solution, and no retro-DA reaction or decomposition occurred, even under heating at 383 K for 24 h. Such stability of Li<sup>+</sup>@C<sub>60</sub>-based DA products stands

### Scheme 1. DA Reaction of [Li<sup>+</sup>@C<sub>60</sub>](PF<sub>6</sub><sup>-</sup>) with 1,3-Cyclohexadiene<sup>a</sup>



<sup>a</sup>10 equiv for preparation and 100 equiv for kinetic measurement.

in marked contrast to the instability of typical DA adducts of empty C<sub>60</sub>. This comparatively high stability is ascribed to the stronger interaction between the lower lying LUMO of Li<sup>+</sup>@C<sub>60</sub> and the HOMO of C<sub>6</sub>H<sub>8</sub> (see Figure 1).<sup>12</sup>

The product was characterized by <sup>1</sup>H, <sup>13</sup>C, and <sup>7</sup>Li NMR, high-resolution atmospheric pressure chemical ionization time-of-flight (APCI–TOF) mass spectrometry, and single-crystal X-ray structural analysis. The <sup>1</sup>H and <sup>13</sup>C NMR spectra of the product (Supporting Information Figures S1 and S2) were quite similar to those of empty C<sub>60</sub>(C<sub>6</sub>H<sub>8</sub>) and showed that the product had C<sub>s</sub>-symmetry with a [6,6]-addition pattern.<sup>13</sup> The <sup>7</sup>Li NMR spectrum (Supporting Information Figure S3) showed a single sharp signal at -13.5 ppm, indicating that the Li<sup>+</sup> was located within the highly shielded fullerene cage. This signal was shifted slightly upfield compared with that of the starting material, [Li<sup>+</sup>@C<sub>60</sub>](PF<sub>6</sub><sup>-</sup>),<sup>7</sup> because the magnetic field inside the cage is altered in the 6,6-adducts of C<sub>60</sub> derivatives; similar upfield shifts have been reported for <sup>3</sup>He and/or H<sub>2</sub>-encapsulated 6,6-adducts of C<sub>60</sub> derivatives.<sup>14</sup> The high-resolution APCI–TOF mass spectrum showed the formation of a product at *m/z* 807.0773, which was assigned to the molecular ion (M<sup>+</sup>; calcd for C<sub>66</sub>H<sub>8</sub>Li, 807.0786; Supporting Information Figure S4). The UV–vis spectrum of [Li<sup>+</sup>@C<sub>60</sub>(C<sub>6</sub>H<sub>8</sub>)](PF<sub>6</sub><sup>-</sup>) was similar to that of the empty analogue (Supporting Information Figure S5).<sup>13a</sup> Finally, the structure was confirmed by X-ray structural analysis (Figure 2

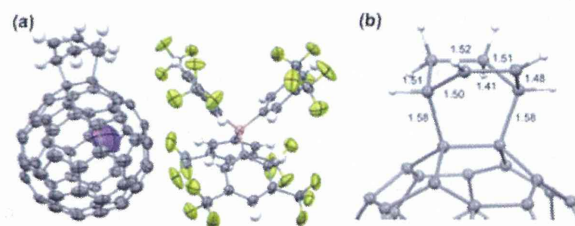


**Figure 2.** Crystal structure of [Li<sup>+</sup>@C<sub>60</sub>(C<sub>6</sub>H<sub>8</sub>)]TFPB<sup>-</sup>: (a) Li<sup>+</sup>@C<sub>60</sub>(C<sub>6</sub>H<sub>8</sub>) cation in the crystal; (b) C<sub>6</sub>H<sub>8</sub> moiety on the fullerene cage (values are C–C bond lengths in angstroms).

and Supporting Information Table S1) after exchanging PF<sub>6</sub><sup>-</sup> with tetrakis[3,5-bis(trifluoromethyl)phenyl]borate (TFPB<sup>-</sup>, B[C<sub>6</sub>H<sub>3</sub>(CF<sub>3</sub>)<sub>2</sub>]<sub>4</sub><sup>-</sup>) by our reported procedure.<sup>15</sup> The crystal structure showed that the addition of C<sub>6</sub>H<sub>8</sub> to the C<sub>60</sub> cage occurred at the [6,6]-bond, as has been discussed in quantum mechanical studies.<sup>16</sup> The encapsulated Li<sup>+</sup> was located close to a six-membered ring near one of the C<sub>6</sub>H<sub>3</sub>(CF<sub>3</sub>)<sub>2</sub> groups of the TFPB counteranion.<sup>7a</sup>

**Kinetics of the DA Reaction of Li<sup>+</sup>@C<sub>60</sub> with 1,3-Cyclohexadiene.** We studied the kinetics of the DA reaction under pseudo-first-order conditions, using a large excess of

$C_6H_8$  (100 equiv) at 253, 263, and 273 K for  $Li^+@C_{60}$  in dichloromethane ( $CH_2Cl_2$ ) and at 353, 363, and 373 K for empty  $C_{60}$  in *o*-dichlorobenzene (*o*-DCB). Different solvents were used due to temperature limitations. We confirmed that empty  $C_{60}$  exhibited no remarkable difference in kinetics between the solvents (measured at 303 K, Supporting Information Table S3). The representative HPLC profile of the DA reaction between  $Li^+@C_{60}$  and  $C_6H_8$  in  $CH_2Cl_2$  is shown in Figure 3. The second-order rate constant  $k_2$  was

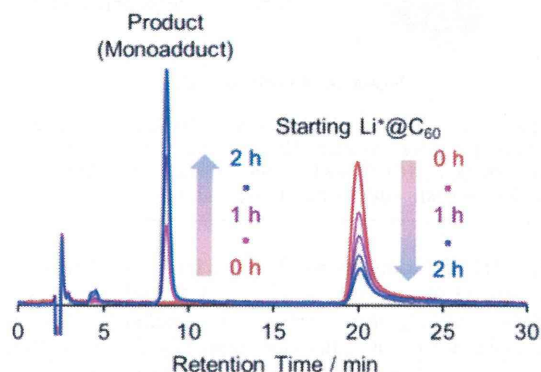


**Figure 3.** Representative HPLC profile (Buckyprep, *o*-DCB/MeCN = 9/1 with 50 mM  $nBu_4NPF_6$ , 1 mL/min) of the DA reaction of  $[Li^+@C_{60}](PF_6^-)$  with 1,3-cyclohexadiene in  $CH_2Cl_2$  at 263 K in the dark.

calculated by using the measured pseudo-first-order rate constant  $k'$  (Supporting Information Figure S6) from the HPLC data, according to the following equation:<sup>17</sup>

$$-d[Li^+@C_{60}]/dt = k'[Li^+@C_{60}] = k_2[Li^+@C_{60}][C_6H_8]$$

The  $k_2$  values at various temperatures are listed in Table 1 along with the  $k_2$  values estimated at 303 K by extrapolation in

**Table 1.** Second-Order Rate Constants for DA Reactions of  $[Li^+@C_{60}](PF_6^-)$  and Empty  $C_{60}$  with  $C_6H_8$

$[Li^+@C_{60}](PF_6^-)$		empty $C_{60}$	
Temp./K	$10^5 k_2 / M^{-1} s^{-1}$	Temp./K	$10^5 k_2 / M^{-1} s^{-1}$
253	1344	353	1187
263	3129	363	2167
273	6714	373	4302
303	52300 <sup>a</sup>	303	21.3 <sup>a</sup>

<sup>a</sup>Estimated by extrapolation in Arrhenius plot.

Arrhenius plots (Figure 4). The  $k_2$  ratio ( $Li^+@C_{60}$  vs  $C_{60}$  at 303 K) revealed that the DA reaction of  $[Li^+@C_{60}](PF_6^-)$  was about 2400-fold faster than the reaction of empty  $C_{60}$ . This difference can be attributed to the encapsulated  $Li^+$ . Using the kinetics data, we computed the activation energy  $E_a$ , activation enthalpy  $\Delta H^\ddagger$ , activation entropy  $\Delta S^\ddagger$ , and activation Gibbs free energy  $\Delta G^\ddagger$  from Arrhenius plots ( $\ln k_2$  vs  $1/T$ ) and Eyring plots ( $\ln(k_2/T)$  vs  $1/T$ ) (see Table 2 and Figure 4) by using the following equations, respectively:<sup>18</sup>

$$\ln k_2 = -E_a/RT + \ln A$$

$$\ln(k_2/T) = -\Delta H^\ddagger/RT + [\ln(k_B/h) + \Delta S^\ddagger/R]$$

Here,  $\ln A$  is a constant,  $k_B$  is the Boltzmann constant, and  $h$  is the Planck constant. Because the DA reaction is bimolecular,

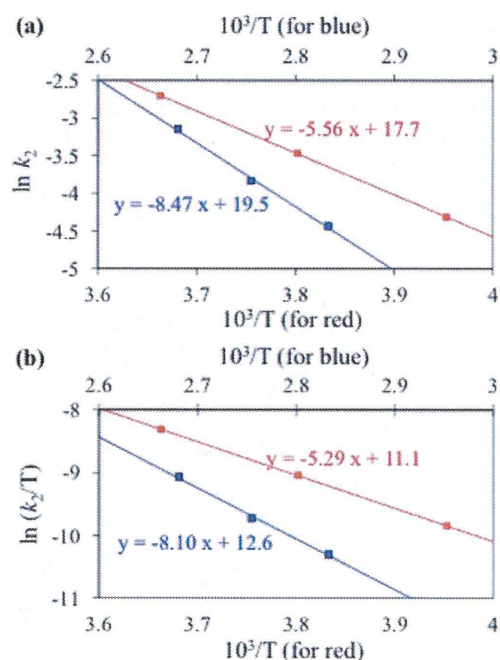


**Figure 4.** (a) Arrhenius and (b) Eyring plots in the DA reaction of  $[Li^+@C_{60}](PF_6^-)$  (red) and empty  $C_{60}$  (blue) with 1,3-cyclohexadiene.

**Table 2.** Activation Parameters for DA Reactions of  $[Li^+@C_{60}](PF_6^-)$  and Empty  $C_{60}$  with  $C_6H_8$

	$E_a$ kJ mol <sup>-1</sup>	$\Delta H^\ddagger$ kJ mol <sup>-1</sup>	$\Delta S^\ddagger$ J mol <sup>-1</sup> K <sup>-1</sup>	$\Delta G^\ddagger$ <sup>a</sup> kJ mol <sup>-1</sup>
$Li^+@C_{60}$	46.2	44.0 (43.6) <sup>b</sup>	-381	144
empty $C_{60}$	70.4	67.4 (65.2) <sup>b</sup>	-368	201

<sup>a</sup>The activation free energies  $\Delta G^\ddagger$  were estimated from each  $\Delta H^\ddagger$ ,  $\Delta S^\ddagger$ , and temperature  $T$  (263 K for  $Li^+@C_{60}$  and 363 K for empty  $C_{60}$ ). <sup>b</sup>Calculated value at M06-2X/6-31G(d) level as *E* (thermal) at 298 K.

$\Delta S^\ddagger$  is negative. However, there was no entropic difference between  $Li^+@C_{60}$  and empty  $C_{60}$ . The observed  $E_a$  value for the DA reaction of  $Li^+@C_{60}$  with  $C_6H_8$  (46.2 kJ mol<sup>-1</sup>) was about 24 kJ mol<sup>-1</sup> lower than that for the reaction of empty  $C_{60}$  (70.4 kJ mol<sup>-1</sup>). This was mainly because the lower LUMO level of  $Li^+@C_{60}$  strengthened the FMO interactions, which is a well-known phenomenon in LA-mediated DA reactions,<sup>2</sup> and we therefore attribute the observed rate enhancement to a similar effect of encapsulated  $Li^+$ . In general, the dominant factors in the rate constant of DA reactions are the energy difference between the HOMO of the diene and the LUMO of dienophile and the steric environment surrounding the FMOs of the diene and dienophile.<sup>5d</sup>

In our experiment, because  $Li^+@C_{60}$  and empty  $C_{60}$  have a [60]fullerene cage of nearly identical size, steric effects do not produce any difference in kinetic behavior. The present reaction is a rare example where we can discuss electronic effects alone in regard to the DA reaction rate, without considering steric effects. Furthermore, in this reaction, the encapsulated  $Li^+$  is considered to be an *intramolecular catalyst*,<sup>11a</sup> which is also a rare example showing the effect of

encapsulation of an LA catalyst rather than coordination to a heteroatom.

**Computational Studies on the DA Reaction of  $\text{Li}^+\text{@C}_{60}$  with 1,3-Cyclohexadiene.** The observed rate enhancement of the DA reaction was in good agreement with the results of DFT calculation at the M06-2X/6-31G(d) level including Grimme's dispersion correction<sup>19</sup> (Figure 5). As reported by

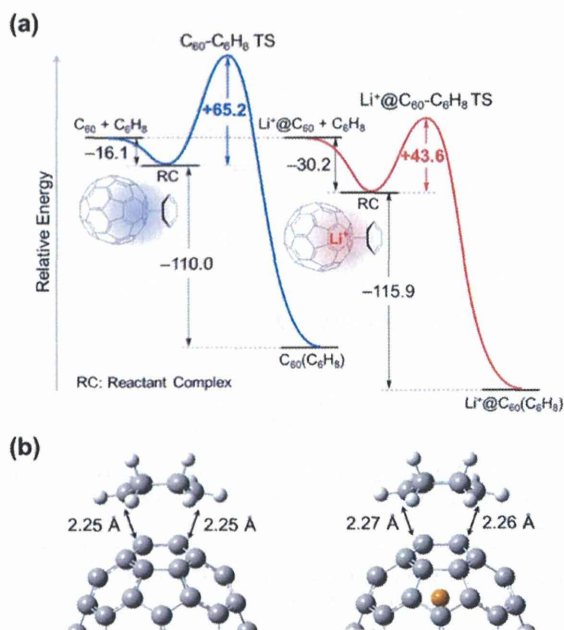


**Figure 5.** (a) Energy profiles (in  $\text{kJ mol}^{-1}$ ) for the DA reaction of empty  $\text{C}_{60}$  (blue) and  $\text{Li}^+\text{@C}_{60}$  (red) with  $\text{C}_6\text{H}_8$  calculated by DFT (M06-2X/6-31G(d)). (b) Transition state structures of  $\text{C}_{60}\text{-C}_6\text{H}_8$  (left) and  $\text{Li}^+\text{@C}_{60}\text{-C}_6\text{H}_8$  systems (right).

Osuna et al.,<sup>16b,19</sup> both  $\text{C}_{60}$  and  $\text{Li}^+\text{@C}_{60}$  form somewhat stable intermediate reactant complexes (RCs) with  $\text{C}_6\text{H}_8$ . Here, the calculated energy difference between the RC and transition state (TS) indicated that the activation energy for the DA reaction of  $\text{Li}^+\text{@C}_{60}$  was  $21.6 \text{ kJ mol}^{-1}$  lower than that of empty  $\text{C}_{60}$ . The calculated activation energy  $E(\text{thermal})$  of  $65.2 \text{ kJ mol}^{-1}$  for  $\text{C}_{60}$  and  $43.6 \text{ kJ mol}^{-1}$  for  $\text{Li}^+\text{@C}_{60}$  agreed fairly well with the experimental values shown in Table 2:  $67.4$  and  $44.0 \text{ kJ mol}^{-1}$ , respectively. The values calculated by using the B3LYP/6-31G\* level of theory without considering the RC were overestimated as  $91$  and  $56 \text{ kJ mol}^{-1}$  (see Supporting Information Figure S7).

In addition, the calculated energy difference between the substrates and the products suggested further stabilization of  $\text{Li}^+\text{@C}_{60}(\text{C}_6\text{H}_8)$ , being explained by the energy gained in orbital interactions,  $\Delta E$ , according to Klopman–Salem equation:<sup>12</sup>

$$\begin{aligned} \Delta E &= 2(C_a C_b \beta_{ab})^2 / |e_a - e_b| \\ &= \text{constant} \times (C_a C_b)^2 / |e_a - e_b| \end{aligned}$$

Here,  $C_a C_b$  denotes the overlap of molecular orbital coefficients of interacting atomic orbitals. The term  $\beta_{ab}$  is the resonance integral that converts the efficiency of overlap to units of energy. Figure 6 shows calculated LUMO energy ( $e_a$ ) of each fullerene and the HOMO energy ( $e_b$ ) of cyclohexadiene (M06-

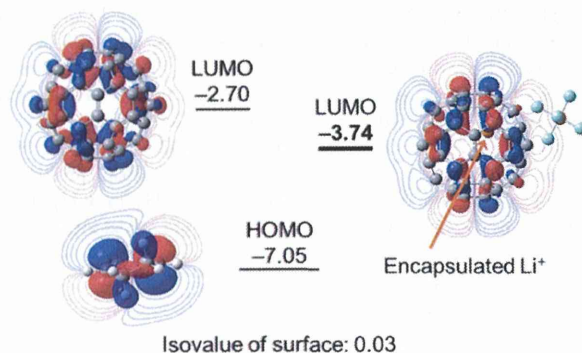


**Figure 6.** Calculated LUMOs of  $\text{Li}^+\text{@C}_{60}$  (with  $\text{PF}_6^-$  counteranion) and empty  $\text{C}_{60}$ , and calculated HOMO of  $\text{C}_6\text{H}_8$  with energies (eV) at the M06-2X/6-31G(d) level. Contour lines in the figure indicate isovalues of 0.001, 0.002, 0.004, 0.008, and 0.02 from the outer side.

2X/6-31G(d) along with schematic images of their orbitals. Because  $\text{Li}^+\text{@C}_{60}$  has a lower LUMO level (closer to the HOMO of  $\text{C}_6\text{H}_8$ ) than empty  $\text{C}_{60}$ , thus making the term  $|e_a - e_b|$  smaller for  $\text{Li}^+\text{@C}_{60}$  than for empty  $\text{C}_{60}$ ,  $\Delta E$  is increased to give a more stabilized TS and product in the case of  $\text{Li}^+\text{@C}_{60}(\text{C}_6\text{H}_8)$ , as shown in Figure 5 ( $115.9 \text{ kJ mol}^{-1}$  from the RC and  $146.1 \text{ kJ mol}^{-1}$  from the starting material). In the case of empty  $\text{C}_{60}$ , these values are somewhat smaller:  $110.0$  and  $126.1 \text{ kJ mol}^{-1}$ , respectively. The reason for the formation of the more stable RC from  $\text{Li}^+\text{@C}_{60}$  than from  $\text{C}_{60}$  is also attributable to the same FMO interactions.

As shown in Figure 6, the slightly delocalized LUMO of  $\text{Li}^+\text{@C}_{60}$ , and thus its increased LUMO coefficient  $C$ , could be another factor in increasing  $\Delta E$ . The slightly increased partial charges in the RC and TS ( $\delta^-$  at the electron-accepting fullerene carbon and  $\delta^+$  at the electron-donating  $\text{C}_6\text{H}_8$  carbon) could be stabilized by the inner  $\text{Li}^+$  of  $\text{Li}^+\text{@C}_{60}$ . This may be the reason that  $\text{C}_6\text{H}_8$  approaches  $\text{Li}^+\text{@C}_{60}$  from the  $\text{Li}^+$  side in the TS (Figure 5). These electronic effects can be quantitatively discussed when steric effect can be completely ignored. In the present comparison of DA kinetics, our system is clearly the ideal case where only electronic effects need to be considered and steric effects can be ignored.

## CONCLUSION

In summary, we have synthesized and characterized a new  $\text{Li}^+$ -encapsulated fullerene derivative [ $\text{Li}^+\text{@C}_{60}(\text{C}_6\text{H}_8)$ ]( $\text{PF}_6^-$ ) obtained by the DA reaction of [ $\text{Li}^+\text{@C}_{60}$ ]( $\text{PF}_6^-$ ) with 1,3-cyclohexadiene. Our study of the DA reaction kinetics revealed that  $\text{Li}^+\text{@C}_{60}$  reacted about 2400 times faster than empty  $\text{C}_{60}$ , because of the stronger interaction between the lower-lying LUMO of  $\text{Li}^+\text{@C}_{60}$  with the HOMO of cyclohexadiene. This remarkable rate enhancement was explained by encapsulated  $\text{Li}^+$  lowering the activation energy by  $24 \text{ kJ mol}^{-1}$ , as estimated from Arrhenius plots. Values of other kinetic parameters, namely, activation enthalpy  $\Delta H^\ddagger$ , activation entropy  $\Delta S^\ddagger$ , and activation Gibbs free energy  $\Delta G^\ddagger$ , were obtained from Eyring plots. The observed rate enhancement caused by encapsulated  $\text{Li}^+$  was supported by DFT calculation at the M06-2X/6-31G(d) level of theory considering RCs with dispersion corrections. The calculation results suggest that encapsulation of  $\text{Li}^+$  lowered the activation energy by  $21.6 \text{ kJ mol}^{-1}$ , which was consistent with the experimental value. The activation energy was lowered through stabilization of the RC and the [4

+ 2] product by 14.1 and 5.9 kJ mol<sup>-1</sup>, respectively. We conclude that encapsulated Li<sup>+</sup> clearly caused the drastic rate enhancement. In this study, we have successfully examined the relation between the HOMO<sub>diene</sub>–LUMO<sub>dienophile</sub> energy gap and DA reaction rate, while isolating the electronic effects and excluding the steric effects.

## EXPERIMENTAL SECTION

**General Procedure.** [Li<sup>+</sup>@C<sub>60</sub>](PF<sub>6</sub><sup>-</sup>) was obtained from Idea International Corporation. All other reagents were commercially available and used without further purification. High resolution mass spectra were obtained by APCI using a TOF mass analyzer on a JEOL JMS-T100LC (AccuTOF) spectrometer with a calibration standard of polyethylene glycol (MW 1000). The <sup>7</sup>Li, <sup>1</sup>H, and <sup>13</sup>C NMR spectra were recorded at 233.12, 599.85, and 150.84 MHz on a Varian Unity Inova 600. UV–vis spectra were recorded on a Shimadzu UV-1800 spectrometer.

**Synthesis of [Li<sup>+</sup>@C<sub>60</sub>(C<sub>6</sub>H<sub>8</sub>)](PF<sub>6</sub><sup>-</sup>).** 1,3-Cyclohexadiene (dichloromethane solution, 53.7 mM, 2 mL, 107 μmol) was slowly added to a dichloromethane solution (47 mL) of [Li<sup>+</sup>@C<sub>60</sub>](PF<sub>6</sub><sup>-</sup>) (9.37 mg, 10.7 μmol) and reacted at 0 °C for 150 min. Then unreacted 1,3-cyclohexadiene was removed in vacuo after dilution of the crude solution by adding chlorobenzene (30 mL) to avoid further progress of the reaction in this process. The product was purified by HPLC at 30 °C using a πNAP (Nacalai Tesque COSMOSIL 4.6 × 250 nm); the mobile phase was chlorobenzene/1,2-dichloroethane/acetonitrile = 2/1.5/6.5 (v/v/v) saturated with Me<sub>4</sub>NPF<sub>6</sub>. After evaporating the solvent in vacuo, dichloromethane was added to the red–brown residue containing white solids of Me<sub>4</sub>NPF<sub>6</sub>. After removing the solids by filtration, recrystallization from the solution by vapor-diffusion with diethyl ether at 0 °C gave brown crystals of [Li<sup>+</sup>@C<sub>60</sub>(C<sub>6</sub>H<sub>8</sub>)]PF<sub>6</sub><sup>-</sup> (1.8 mg, 18%, 1.9 μmol, red–brown solid). <sup>1</sup>H NMR (600 MHz, dichloromethane-*d*<sub>2</sub>): δ 7.34 (dd, *J* = 4.6, 3.2 Hz, 2H, vinyl), 4.26 (m, 2H, bridgehead), 3.10 (m, 2H), 2.31 (m, 2H). <sup>13</sup>C NMR (151 MHz, dichloromethane-*d*<sub>2</sub>): δ 156.88 (s), 156.24 (s), 146.46 (s), 145.54 (s), 145.46 (s), 145.31 (s), 145.28 (s), 145.16 (s), 144.81 (s), 144.49 (s), 144.47 (s), 144.35 (s), 144.07 (s), 143.54 (s), 143.29 (s), 142.43 (s), 142.07 (s), 141.92 (s), 141.07 (s), 140.78 (s), 140.77 (s), 140.68 (s), 140.63 (s), 140.57 (s), 139.00 (s), 138.94 (s), 136.38 (s), 135.40 (s), 135.14 (s), 70.48 (s), 42.87 (s), 24.59 (s). <sup>7</sup>Li NMR (233 MHz, dichloromethane-*d*<sub>2</sub>): δ -13.5 (s). High-resolution APCI-TOF MS (+): *m/z* calcd for C<sub>66</sub>H<sub>8</sub>Li, 807.0786; found, 807.0773.

**X-ray Structural Analysis of [Li<sup>+</sup>@C<sub>60</sub>(C<sub>6</sub>H<sub>8</sub>)]TFPB<sup>-</sup>.** Structural characterization of Li<sup>+</sup>@C<sub>60</sub>(C<sub>6</sub>H<sub>8</sub>) was performed by means of single crystal X-ray diffraction of [Li<sup>+</sup>@C<sub>60</sub>(C<sub>6</sub>H<sub>8</sub>)]TFPB<sup>-</sup>. [Li<sup>+</sup>@C<sub>60</sub>(C<sub>6</sub>H<sub>8</sub>)]PF<sub>6</sub><sup>-</sup> (0.2 mg) and NaTFPB (1.1 mg, excess) were dissolved in 4 mL of dichloromethane with ultrasonic agitation (1 min). Then, the solution was filtered and concentrated in vacuo to ~60 μL. Recrystallization from the solution by vapor-diffusion with diethyl ether at 0 °C gave brown crystals of [Li<sup>+</sup>@C<sub>60</sub>(C<sub>6</sub>H<sub>8</sub>)]TFPB<sup>-</sup>. The synchrotron-radiation X-ray diffraction measurement was performed by using the large cylindrical image-plate camera at SPring-8 BL02B1 (Hyogo, Japan) at 150 K. The crystal structure analysis was performed by using SHELX. The results are summarized in Supporting Information Table S1 and the CIF file (CCDC 985137). The Li<sup>+</sup>@C<sub>60</sub>(C<sub>6</sub>H<sub>8</sub>) crystal showed a disordered structure with two molecular orientations evenly coexisted in the crystal. The encapsulated Li<sup>+</sup> cation is localized under a six-membered ring so that the C<sub>6</sub> symmetry of the molecule is broken in the crystal.

**Kinetic Evaluation in the DA Reactions of [Li<sup>+</sup>@C<sub>60</sub>](PF<sub>6</sub><sup>-</sup>) and Empty C<sub>60</sub> with 1,3-Cyclohexadiene (and Other 1,3-Dienes).** The kinetic measurements for the DA reactions of [Li<sup>+</sup>@C<sub>60</sub>](PF<sub>6</sub><sup>-</sup>) and empty C<sub>60</sub> with 1,3-cyclohexadiene were performed under pseudo-first-order conditions by using a large excess of diene (ca. 100 equiv, 6 mM) relative to fullerenes (ca. 60 μM) in the dark. The progress of the reaction was followed by monitoring the consumption of C<sub>60</sub> by HPLC. For [Li<sup>+</sup>@C<sub>60</sub>](PF<sub>6</sub><sup>-</sup>): column, Buckyprep (Nacalai Tesque COSMOSIL 4.6 × 250 nm); eluent, *o*-dichlorobenzene/acetonitrile = 9/1 (v/v) with saturated <sup>n</sup>Bu<sub>4</sub>NPF<sub>6</sub>;

temperature, RT. For empty C<sub>60</sub>; column: Buckyprep (Nacalai Tesque COSMOSIL 4.6 × 250 nm), eluent: toluene, temperature: RT. Monitoring the reaction by HPLC showed a gradual increase of monoadduct ([Li<sup>+</sup>@C<sub>60</sub>(C<sub>6</sub>H<sub>8</sub>)](PF<sub>6</sub><sup>-</sup>) or empty C<sub>60</sub>(C<sub>6</sub>H<sub>8</sub>)) accompanied by consumption of the starting material. The natural logarithmic plot of the normalized signal intensity of each remaining fullerene starting material (relative to the signal intensity of the first aliquot at *t* = 0) was linear with respect to time. The obtained slope, that is, the pseudo-first-order rate constant *k*'<sub>1</sub>, was divided by the concentration of 1,3-cyclohexadiene to obtain the second-order rate constants *k*'<sub>2</sub>.

**Theoretical Calculation.** Full geometry optimizations have been carried out by using the restricted M06-2X functional with the 6-31G(d) basis set in Gaussian 09 (rev. C.01) software.<sup>20</sup> Frequency calculations showed only one imaginary frequency for the transition states (351i for Li<sup>+</sup>@C<sub>60</sub><sup>+</sup> and 404i for C<sub>60</sub>) or no imaginary frequency for the other states. All energies include zero-point energies (ZPEs) and thermal corrections by the frequency calculations.

## ASSOCIATED CONTENT

### Supporting Information

Crystallographic data (including CIF), kinetic data with various 1,3-dienes and in various solvents, spectroscopic data (NMR, MS, and UV–vis) of the new compound, kinetic plots of the DA reactions, the calculated energy profiles at B3LYP/6-31G\* level, the calculated energies, and the coordinates of the atoms in all the molecules optimized. This material is available free of charge via the Internet at <http://pubs.acs.org>.

## AUTHOR INFORMATION

### Corresponding Authors

\*E-mail: kokubo@chem.eng.osaka-u.ac.jp.

\*E-mail: matsuo@chem.s.u-tokyo.ac.jp.

### Present Address

<sup>†</sup>H. Ueno: JST ERATO Itami Molecular Nanocarbon Project, Graduate School of Science, Nagoya University, Japan.

### Notes

The authors declare no competing financial interest.

## ACKNOWLEDGMENTS

This work was partly supported by Adaptable and Seamless Technology Transfer Program through target-driven R&D, JST, Health Labor Sciences Research Grants from the MHLW of Japan (to K.K.), and the Funding Program for Next-Generation World-Leading Researchers (to Y.M.). The X-ray diffraction measurement was performed at SPring-8 with the approval of the Japan Synchrotron Radiation Research Institute (JASRI) (Proposal No. 2013B0100).

## REFERENCES

- (1) Diels, O.; Alder, K. *Liebigs Ann. Chem.* **1928**, *460*, 98–122.
- (2) Jiang, X.; Wang, R. *Chem. Rev.* **2013**, *113*, 5515–5546.
- (3) (a) Pham, H. V.; Paton, R. S.; Ross, A. G.; Danishefsky, S. J.; Houk, K. N. *J. Am. Chem. Soc.* **2014**, *136*, 2397–2403. (b) Konovalov, A. I.; Kiselev, V. D. *Russ. Chem. Bull., Int. Ed.* **2003**, *52*, 293–311. (c) Sustmann, R.; Schubert, R. *Angew. Chem., Int. Ed.* **1972**, *11*, 840–840.
- (4) (a) Forman, M. A.; Dailey, W. P. *J. Am. Chem. Soc.* **1991**, *113*, 2761–2762. (b) Tsuda, A.; Oshima, T. *New J. Chem.* **1998**, 1027–1029.
- (5) (a) Hudhomme, P. C. R. *Chimie* **2006**, *9*, 881–891. (b) Matsuo, Y.; Kawai, J.; Inada, H.; Nakagawa, T.; Ota, H.; Otsubo, S.; Nakamura, E. *Adv. Mater.* **2013**, *25*, 6266–6269. (c) He, Y.; Chen, H.-Y.; Hou, J.; Li, Y. *J. Am. Chem. Soc.* **2010**, *132*, 1377–1382. (d) Ikuma, N.; Susami, Y.; Oshima, T. *Eur. J. Org. Chem.* **2011**, 6452–6458.

- (6) (a) Schlueter, J. A.; Seaman, J. M.; Taha, S.; Cohen, H.; Lykke, K. R.; Wang, H. H.; Williams, J. M. *J. Chem. Soc., Chem. Commun.* **1993**, 972–974. (b) Komatsu, K.; Murata, Y.; Sugita, N.; Takeuchi, K.; Wan, T. S. M. *Tetrahedron Lett.* **1993**, *34*, 8473–8476. (c) Giovane, L. M.; Barco, J. W.; Yadav, T.; Lafleur, A. L.; Marr, J. A.; Howard, J. B.; Rotello, V. M. *J. Phys. Chem.* **1993**, *97*, 8560–8561.
- (7) (a) Aoyagi, S.; Nishibori, E.; Sawa, H.; Sugimoto, K.; Takata, M.; Miyata, Y.; Kitaura, R.; Shinohara, H.; Okada, H.; Sakai, T.; Ono, Y.; Kawachi, K.; Yokoo, K.; Ono, S.; Omote, K.; Kasama, Y.; Ishikawa, S.; Komuro, T.; Tobita, H. *Nat. Chem.* **2010**, *2*, 678–683. (b) Okada, H.; Komuro, T.; Sakai, T.; Matsuo, Y.; Ono, Y.; Omote, K.; Yokoo, K.; Kawachi, K.; Kasama, Y.; Ono, S.; Hatakeyama, R.; Kaneko, T.; Tobita, H. *RSC Adv.* **2012**, *2*, 10624–10631. (c) Fukuzumi, S.; Ohkubo, K.; Kawashima, Y.; Kim, D. S.; Park, J. S.; Jana, A.; Lynch, V. M.; Kim, D.; Sessler, J. L. *J. Am. Chem. Soc.* **2011**, *133*, 15938–15941. (d) Aoyagi, S.; Sado, Y.; Nishibori, E.; Sawa, H.; Okada, H.; Tobita, H.; Kasama, Y.; Kitaura, R.; Shinohara, H. *Angew. Chem., Int. Ed.* **2012**, *51*, 3377–3381. (e) Ueno, H.; Kokubo, K.; Nakamura, Y.; Ohkubo, K.; Ikuma, N.; Moriyama, H.; Fukuzumi, S.; Oshima, T. *Chem. Commun.* **2013**, *49*, 7376–7378.
- (8) Kawakami, H.; Okada, H.; Matsuo, Y. *Org. Lett.* **2013**, *15*, 4466–4469.
- (9) (a) Murata, M.; Maeda, S.; Morinaka, Y.; Murata, Y.; Komatsu, K. *J. Am. Chem. Soc.* **2008**, *130*, 15800–15801. (b) Frunzi, M.; Xu, H.; Cross, R. J.; Saunders, M. *J. Phys. Chem. A* **2009**, *113*, 4996–4999. (c) Osuna, S.; Swart, M.; Solà, M. *Chem.—Eur. J.* **2009**, *15*, 13111–13123; Osuna, S.; Swart, M.; Solà, M. *Chem.—Eur. J.* **2010**, *16*, 3878–3878. (d) Osuna, S.; Swart, M.; Solà, M. *Phys. Chem. Chem. Phys.* **2011**, *13*, 3585–3603.
- (10) (a) Maeda, Y.; Miyashita, J.; Hasegawa, T.; Wakahara, T.; Tsuchiya, T.; Nakahodo, T.; Akasaka, T.; Mizorogi, N.; Kobayashi, K.; Nagase, S.; Kato, T.; Ban, N.; Nakajima, H.; Watanabe, Y. *J. Am. Chem. Soc.* **2005**, *127*, 12190–12191. (b) Garcia-Borràs, M.; Luis, J. M.; Swart, M.; Solà, M. *Chem.—Eur. J.* **2013**, *19*, 4468–4479. (c) Sato, S.; Maeda, Y.; Guo, J.-D.; Yamada, M.; Mizorogi, N.; Nagase, S.; Akasaka, T. *J. Am. Chem. Soc.* **2013**, *135*, 5582–5587.
- (11) (a) Matsuo, Y.; Okada, H.; Maruyama, M.; Sato, H.; Tobita, H.; Ono, Y.; Omote, K.; Kawachi, K.; Kasama, Y. *Org. Lett.* **2012**, *14*, 3784–3787. (b) Ueno, H.; Nakamura, Y.; Ikuma, N.; Kokubo, K.; Oshima, T. *Nano Res.* **2012**, *5*, 558–564. (c) Ueno, H.; Kokubo, K.; Kwon, E.; Nakamura, Y.; Ikuma, N.; Oshima, T. *Nanoscale* **2013**, *5*, 2317–2321.
- (12) (a) Klopman, G. *J. Am. Chem. Soc.* **1968**, *90*, 223–234. (b) Salem, L. *J. Am. Chem. Soc.* **1968**, *90*, 543–552.
- (13) (a) Kräutler, B.; Maynollo, J. *Tetrahedron* **1996**, *52*, 5033–5042. (b) Kräutler, B.; Müller, T.; Maynollo, J.; Gruber, K.; Kratky, C.; Ochsenbein, C.; Schwarzenbach, D.; Bürgi, H.-B. *Angew. Chem., Int. Ed. Engl.* **1996**, *35*, 1204–1206.
- (14) (a) Saunders, M.; Cross, R. J.; Jiménez-Vázquez, H. A.; Shimshi, R.; Khong, A. *Science* **1996**, *271*, 1693–1697. (b) Murata, M.; Murata, Y.; Komatsu, K. *J. Am. Chem. Soc.* **2006**, *128*, 8024–8033.
- (15) Okada, H.; Matsuo, Y. *Fullerenes, Nanotubes, Carbon Nanostruct.* **2014**, *22*, 262–268.
- (16) (a) Osuna, S.; Morera, J.; Cases, M.; Morokuma, K.; Solà, M. *J. Phys. Chem. A* **2009**, *113*, 9721–9726. (b) Fernandez, I.; Solà, M.; Bickelhaupt, F. M. *Chem.—Eur. J.* **2013**, *19*, 7416–7422.
- (17) Oshima, T.; Kitamura, H.; Higashi, T.; Kokubo, K.; Seike, N. *J. Org. Chem.* **2006**, *71*, 2995–3000.
- (18) (a) Eyring, H. *J. Chem. Phys.* **1935**, *3*, 107–115. (b) Pross, A. In *Theoretical and Physical Principles of Organic Reactivity*; John Wiley & Sons, Inc.: New York, 1995; pp 130–133.
- (19) Osuna, S.; Marcel, S.; Solà, M. *J. Phys. Chem. A* **2011**, *115*, 3491–3496.
- (20) Frisch, M. J.; Trucks, G. W.; Schlegel, H. B.; Scuseria, G. E.; Robb, M. A.; Cheeseman, J. R.; Scalmani, G.; Barone, V.; Mennucci, B.; Petersson, G. A.; Nakatsuji, H.; Caricato, M.; Li, X.; Hratchian, H. P.; Izmaylov, A. F.; Bloino, J.; Zheng, G.; Sonnenberg, J. L.; Hada, M.; Ehara, M.; Toyota, K.; Fukuda, R.; Hasegawa, J.; Ishida, M.; Nakajima, T.; Honda, Y.; Kitao, O.; Nakai, H.; Vreven, T.; Montgomery, Jr., J. A.;

## Research Article

# Systematic Evaluation and Mechanistic Investigation of Antioxidant Activity of Fullerenols Using $\beta$ -Carotene Bleaching Assay

Hiroshi Ueno, Shizuka Yamakura, Riya S. Arastoo, Takumi Oshima, and Ken Kokubo

Division of Applied Chemistry, Graduate School of Engineering, Osaka University, 2-1 Yamadaoka, Suita, Osaka Prefecture 565-0871, Japan

Correspondence should be addressed to Ken Kokubo; kokubo@chem.eng.osaka-u.ac.jp

Received 27 June 2014; Accepted 12 August 2014; Published 28 August 2014

Academic Editor: Naoki Kishi

Copyright © 2014 Hiroshi Ueno et al. This is an open access article distributed under the Creative Commons Attribution License, which permits unrestricted use, distribution, and reproduction in any medium, provided the original work is properly cited.

Antioxidant activity of hydroxylated fullerenes, so-called fullerenols, against lipid peroxyl radical was evaluated by  $\beta$ -carotene bleaching assay. All samples showed moderate to high antioxidant activity (%AOA), especially for  $C_{60}(OH)_{12}$  (70.1) and  $C_{60}(OH)_{44}$  (66.0) as compared with 8, 24, 26, and 36 hydroxylated ones (31.7–62.8). The detection of the possible products was conducted in the model reaction of both fullerenols and  $C_{60}$  with methyl linoleate by MALDI-TOF-MS. These results suggested that the two possible mechanisms, such as C-addition to double bonds and H-abstraction from –OH groups, are involved in the present radical scavenging reaction.

## 1. Introduction

Fullerene known as “radical sponge” has been recognized as a new class of antioxidant due to its high reactivity toward radical species since its first report in 1991 [1]. Reactive oxygen species (ROS), such as superoxide, hydroxyl radical, peroxyl radicals, and nitric oxide, have such radical nature and cause damage to biomolecules, including DNA, cell, protein, and lipid, inducing various diseases. For this reason, the development of biocompatible, nontoxic, and water-soluble fullerene derivatives has been strongly demanded. In the past several years, we have evaluated the ROS radical scavenging ability as “antioxidant activity” of water-soluble  $\gamma$ -cyclodextrin- (CD-) bicapped  $C_{60}$  and polyvinylpyrrolidone- (PVP-) entrapped  $C_{60}$  as well as the corresponding fullerene oxides ( $C_{60}O_n$ ) [2, 3]. However, their solubility in water still remains low and inevitable steric repulsion from the host compounds, such as CD and PVP, brings about undesirable interference for accurate bioassay.

Polyhydroxylated fullerenes, so-called fullerenols, have attracted much attention in view of biological, pharmaceutical, and medical applications, because of their high hydrophilicity and the low toxicity as well as the unique

spherical structure with a diameter of ca. 1 nm. In this point of view, the antioxidant activity of fullereneol has been reported in 1995 by Chiang et al. for  $C_{60}(OH)_{12}$  [4] and in 2009 by Miwa et al. for highly hydroxylated fullereneol  $C_{60}(OH)_{32}$  [5] as well as other bioactivities, such as the inhibitive effect for oxidative stress in adipocytes [6], protective effect of human keratinocytes from UV-induced cell injuries [7], and suppression of intracellular lipid accumulation [8]. In connection with the recent developments of these biological studies [9–11], new and facile synthetic procedures of highly hydroxylated water-soluble fullerenols have been reported [12–14]. However, little is known about their origin of antioxidant activity and the relationship between the activity and the number of hydroxyl groups. For the development of new application of these unique nanomaterials, the systematic investigation of the antioxidant activity of variously hydroxylated fullerenols, such as 8, 10, 12, 24, 26, 36, and 44 hydroxylated ones [15], is highly desirable to explore the antioxidant mechanism of fullerenols toward ROS (Figure 1).

The  $\beta$ -carotene bleaching assay for evaluating antioxidant activity is one of the common methods used in the field of food chemistry [16]. The principle of the method is based on the discoloration of yellowish color of a  $\beta$ -carotene solution

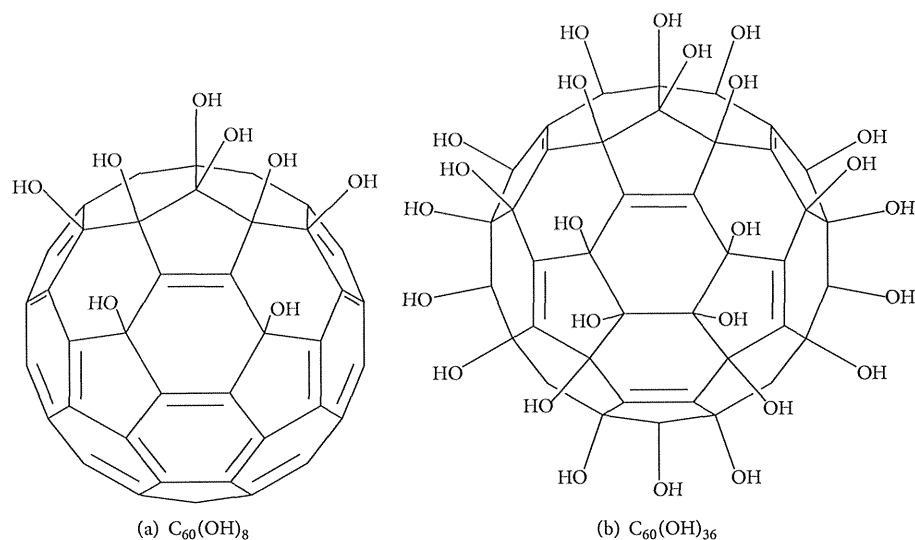


FIGURE 1: A possible isomer of fullerlenols composed of a mixture of isomers and expressed by the average structures as (a)  $C_{60}(OH)_8$  and (b)  $C_{60}(OH)_{36}$ .

due to the breaking of  $\pi$ -conjugation by addition reaction of lipid or lipid peroxy radical ( $L^*$  or  $LOO^*$ ) to a C=C double bond of  $\beta$ -carotene. The radical species is generated from the autoxidation of linoleic acid by heating under air atmosphere. When the appropriate antioxidant is added to the solution, the discoloration can be retarded by competing reaction between  $\beta$ -carotene and antioxidant with the subjected radicals. The structural similarity between fullerenes and  $\beta$ -carotene, such as highly  $\pi$ -conjugated molecules, enables the accurate evaluation of antioxidant activity by this  $\beta$ -carotene bleaching assay in contrast to other methods like DPPH radical assay [17].

Herein, we report the systematic investigation of antioxidant activity of variously hydroxylated fullerlenols with 8, 10, 12, 24, 26, 36, and 44 hydroxyl groups evaluated by  $\beta$ -carotene bleaching assay. In combination with detecting the possible products of both fullerlenols and  $C_{60}$  with radical species generated from methyl linoleate under autoxidation condition, we propose two antioxidant mechanisms which are dependent on the number of hydroxyl groups.

## 2. Materials and Methods

**2.1. Materials and Apparatuses.** Fullerlenols  $C_{60}(OH)_n$  ( $n = 44$  and 36) were synthesized by the previously reported procedures using hydrogen peroxide [12, 13] and  $C_{60}(OH)_{26}$  was synthesized by the modified method with a shorter reaction time (methods A and A'). Fullerenol  $C_{60}(OH)_{24}$  prepared from  $C_{60}Br_{24}$  was purchased from MTR Ltd. (method B). Fullerlenols  $C_{60}(OH)_n$  ( $n = 12$  and 8) were synthesized by the modification of the literature method using oleum (method C) [19]. Fullerene  $C_{60}$  was purchased from Frontier Carbon Corporation as nanom purple ST (99%).

$\beta$ -Carotene, linoleic acid (>99%), catechin mixture, isoflavone mixture, coenzyme Q10 (as ubiquinone-10),

curcumin, and  $\alpha$ -lipoic acid were purchased from Wako Pure Chemical Industries, Ltd. Other reagents and organic solvents as well as pure water were all commercially available and used as received. UV-visible spectra were measured on a JASCO V-550 equipped with a thermal controller. LCMS analysis was performed on a SHIMADZU LCMS-2010EV. Matrix assisted laser desorption ionization time-of-flight mass spectra (MALDI-TOF-MS) were measured on a Bruker autoflex III.

**2.2.  $\beta$ -Carotene Bleaching Assay.** The  $\beta$ -carotene bleaching assay was performed according to an optimally modified procedure [2, 3]. Chloroform solutions of 11  $\mu$ L of  $\beta$ -carotene (1.0 mg/mL, 8.2  $\mu$ M), 4.4  $\mu$ L of linoleic acid (0.1 g/mL, 628  $\mu$ M), and 22  $\mu$ L of Tween 40 (0.2 g/mL) were mixed in a quartz cell equipped with a screw-on cap and then the solvent was removed in vacuo. The residual emulsion was immediately diluted with 2.4 mL of phosphate buffer solution (0.02 M, pH = 7.01), and 0.1 mL of antioxidant (0–20  $\mu$ M) in deionized water ( $C_{60}(OH)_{24}$ , 36, and 44) or DMSO ( $C_{60}(OH)_8$ , 12, and 26) was added to the diluted mixture. The solution was mixed well and heated at 50°C under air in a quartz cell on a UV spectrometer in order to monitor the decrease in the absorbance of  $\beta$ -carotene at 460 nm.

## 3. Results and Discussion

The discoloration rate in the presence of fullerene ( $R_f$ ) is defined as (1), where  $k_{obs}$  is an observed pseudo-first-order rate constant, and  $k_c$  and  $k_f$  are rate constants for the reaction of  $\beta$ -carotene and fullerene with radical species (represented by  $LOO^*$ ), respectively. Because the concentration of radical species must be considerably low and if it is approximated as a constant, the rate obeys a pseudo-first-order rate law with a constant of  $k_{obs}$ . When fullerene is absent as a control (i.e.,

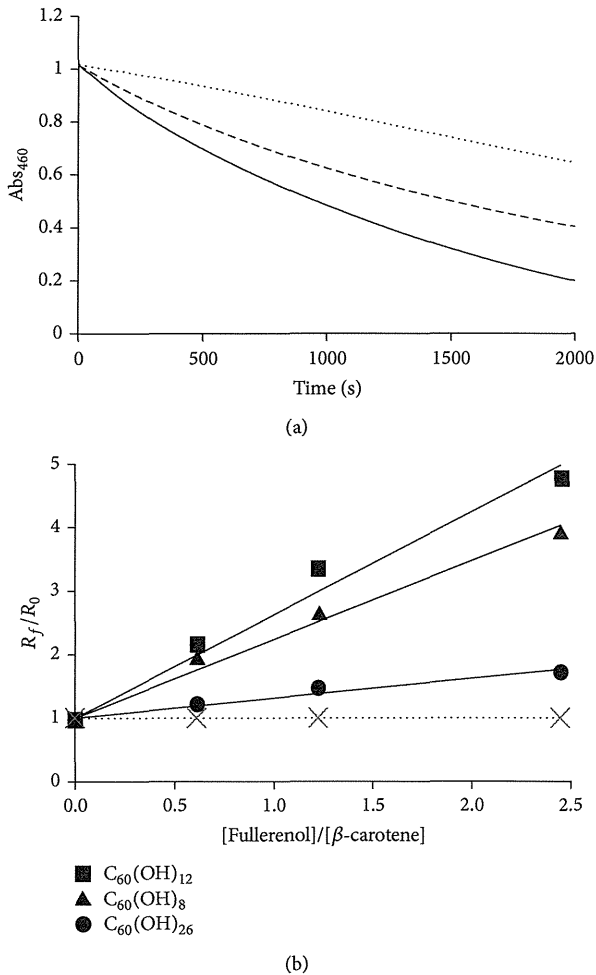


FIGURE 2: (a) Time course of the discoloration of  $\beta$ -carotene induced by autoxidation of linoleic acid under air at  $50^\circ\text{C}$  in the absence (solid line for control) or the presence of fullerenols (dotted line for  $\text{C}_{60}(\text{OH})_{12}$  and dashed line for  $\text{C}_{60}(\text{OH})_8$  in  $10\ \mu\text{M}$ ) by monitoring of UV absorbance at 460 nm. (b) Plots of the ratio of  $\beta$ -carotene bleaching (discoloration) rates in the presence ( $R_f$ ) or absence ( $R_0$ ) of fullereneol  $R_f/R_0$  versus the ratio of concentration  $[\text{fullerene}]/[\beta\text{-carotene}]$  for various fullerenols: marked by square for  $\text{C}_{60}(\text{OH})_{12}$ , triangle for  $\text{C}_{60}(\text{OH})_8$ , and circle for  $\text{C}_{60}(\text{OH})_{26}$ . The slope of each linear regression line corresponds to the relative radical scavenging rate constant  $k_{\text{rel}}$  of fullerenols relative to  $\beta$ -carotene ( $=k_f/k_c$ ). The dotted horizontal line indicates the value in the absence of antioxidant as a control ( $R_f = R_0$  at any concentration;  $k_{\text{rel}} = 0$ ).

$[\text{fullerene}] = 0$ ), the discoloration rate of  $\beta$ -carotene is defined as  $R_0$ . Consider

$$\begin{aligned} R_f &= \frac{-d[\beta\text{-carotene}]}{dt} = k_{\text{obs}}[\beta\text{-carotene}] \\ &= k_c[\beta\text{-carotene}] \\ &\quad \times \left( \frac{k_c[\beta\text{-carotene}]}{k_c[\beta\text{-carotene}] + k_f[\text{fullerene}]} \right) [\text{LOO}^*]. \end{aligned} \quad (1)$$

TABLE 1: The relative rate constant ( $k_{\text{rel}}$ ) and antioxidant activity (%AOA) of fullerenols<sup>a</sup>.

Compound	Method <sup>b</sup>	$k_{\text{rel}}$	%AOA at $10\ \mu\text{M}$
$\text{C}_{60}(\text{OH})_{44}$	A	1.54	66.0
$\text{C}_{60}(\text{OH})_{36}$	A'	0.80	52.7
$\text{C}_{60}(\text{OH})_{24}$	B	0.68	46.0
$\text{C}_{60}(\text{OH})_{26}$	A'	0.31	31.7
$\text{C}_{60}(\text{OH})_{12}$	C	1.62	70.1
$\text{C}_{60}(\text{OH})_8$	C	1.24	62.8
$\text{C}_{60}$ <sup>c</sup>	[3]	0.79	50.0

<sup>a</sup>The reaction was conducted in anoxic conditions.

<sup>b</sup>Preparation method described in Section 2.

<sup>c</sup>PVP was used as a water solubilizer.

The  $\beta$ -carotene bleaching assay was carried out by previously reported method [2]. The decrease in absorbance of  $\beta$ -carotene is plotted as  $\ln[(\text{Abs}_0)/(\text{Abs}_t)]$  versus reaction time that gave a linear regression line after a short presteady state (Figure 2(a)), consistent with the above approximation of the reaction as a pseudo-first-order kinetics (1).

By the plot of discoloration rate ratio  $R_f/R_0$  to the various molar ratio of  $[\text{fullerene}]/[\beta\text{-carotene}]$  as shown in Figure 2(b), the ratio of rate constants  $k_f/k_c$ , which means the relative reactivity of fullerene to  $\beta$ -carotene (defined as  $k_{\text{rel}}$ ), can be obtained as the slope of a linear line with the intercept of 1 as expressed by

$$\begin{aligned} \frac{R_f}{R_0} &= \frac{k_{\text{obs}} \text{ of fullerene}}{k_{\text{obs}} \text{ of control}} = \frac{k_c[\beta\text{-carotene}] + k_f[\text{fullerene}]}{k_c[\beta\text{-carotene}]} \\ &= 1 + \frac{k_f}{k_c} \frac{[\text{fullerene}]}{[\beta\text{-carotene}]}, \quad \left( \frac{k_f}{k_c} = k_{\text{rel}} \right). \end{aligned} \quad (2)$$

The  $R_f/R_0$  plots for  $\text{C}_{60}(\text{OH})_8$ ,  $\text{C}_{60}(\text{OH})_{12}$ , and  $\text{C}_{60}(\text{OH})_{26}$  exhibited that the highest  $k_{\text{rel}}$  value of 1.62 (i.e., 1.62 times reactive toward the present radical species relative to  $\beta$ -carotene) was observed for  $\text{C}_{60}(\text{OH})_{12}$ . The  $k_{\text{rel}}$  values as well as %AOA at  $10\ \mu\text{M}$  of various fullerenols were summarized in Table 1. The antioxidant activity expressed using %AOA was defined by (3). The fullerenols having higher  $k_{\text{rel}}$  values showed higher values of %AOA. The %AOA is convenient to express the antioxidant activity using the value in the range from 0 (low) to 100 (high). However, it should be noted that the value of %AOA is concentration-dependent and the value of  $k_{\text{rel}}$  is not. Consider

$$\% \text{AOA} = \frac{(k_{\text{obs}} \text{ of control}) - (k_{\text{obs}} \text{ of sample})}{k_{\text{obs}} \text{ of control}} \times 100. \quad (3)$$

Fullerenols  $\text{C}_{60}(\text{OH})_n$  having ca. 10 ( $n = 8$  and 12) or ca. 40 (36 and 44) hydroxyl groups showed somewhat high antioxidant activity as compared with those having ca. 25 (24 and 26). Lowly hydroxylated fullerene (ca. 10) showed high antioxidant activity probably because of the remaining relatively high  $\pi$ -conjugation in C=C double bonds, such as high HOMO and low LUMO, which is favourable for the



TABLE 2: The relative rate constant ( $k_{rel}$ ) and antioxidant activity (%AOA) of naturally occurring antioxidants<sup>a,b</sup>.

Compound	$k_{rel}$	%AOA at 10 $\mu$ M
Catechin	4.95	80.2
$C_{60}(OH)_{44}$	1.54	66.0
$\beta$ -Carotene	1.00	—
Isoflavone	0.68	35.6
Coenzyme Q10	0.50	29.1
Curcumin	0.26	17.7
$\alpha$ -Lipoic acid	0.10	7.4

<sup>a</sup>The reaction was conducted in anoxic conditions.

<sup>b</sup>Data from [18].

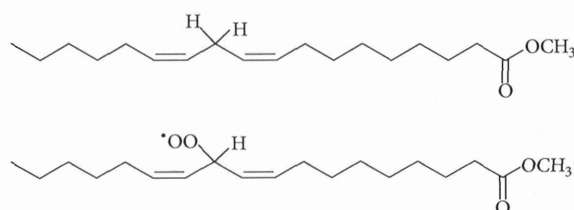
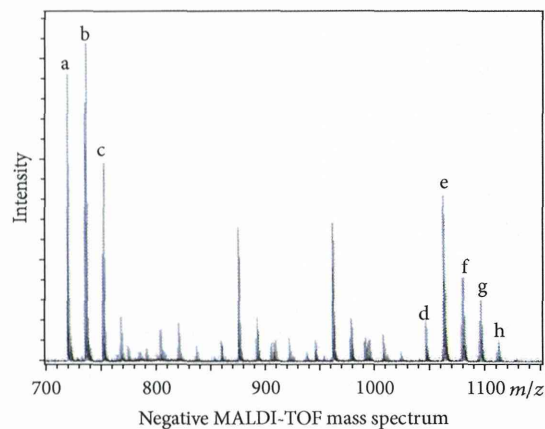


FIGURE 3: Structure of methyl linoleate (ML) and its peroxy radical (MLOO\*).

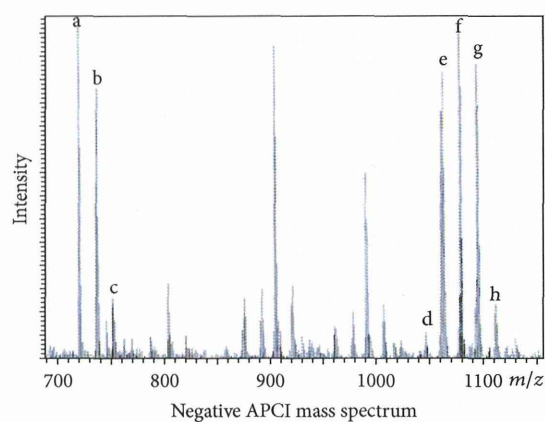
efficient molecular orbital interaction with the radical SOMO. Therefore, the activity decreased with the increasing number of hydroxyl groups, thus decreasing  $\pi$ -conjugation, up to ca. 25. However, surprisingly, the activity again increased with the increasing number of hydroxyl groups up to ca. 40 as highly hydroxylated ones. The present result suggests that the antioxidant mechanism of highly hydroxylated fullerenes may be different from those of lowly hydroxylated ones (vide infra).

For the comparison, the antioxidant activities of representative naturally occurring antioxidants measured by the same procedure were summarized in Table 2 [18]. Catechin showed the extremely high  $k_{rel}$  and %AOA values among those tested. Fullerenol  $C_{60}(OH)_{44}$  also exhibited relatively high radical scavenging activity, slightly higher even than  $\beta$ -carotene, while curcumin and  $\alpha$ -lipoic acid showed poor values in the present  $\beta$ -carotene bleaching assay.

General antioxidants are mainly categorized into three types according to their antioxidant mechanism, such as (i) electron donating type (reductant like ascorbic acid), (ii) hydrogen donating type (antioxidant having reactive hydrogen atom like phenolic -OH group of catechin), and (iii) radical trapping type (antioxidant having highly conjugated C=C double bonds like  $\beta$ -carotene) [20]. To investigate the antioxidant mechanism of fullerene, the reaction of  $C_{60}$  with methyl linoleate (ML) under autoxidation condition [21], heating with 300 equivalent excess of ML in toluene at 70°C for 3 days, was conducted as a model reaction. Because of the technical problems on solubility and mass detectability, the employment of linoleic acid failed. Both by MALDI-TOF-MS and by LC-MS with APCI negative mode analyses of the crude reaction mixture, the peroxy



(a)



(b)

Peak	$m/z$ (MALDI/APCI)	Ion
a	720/720	$C_{60}^-$
b	737/737	$C_{60}(OH)^-$
c	753/753	$C_{60}O(OH)^-$
d	1045/1046	$C_{60}(OOML)^-$
e	1061/1062	$C_{60}O(OOML)^-$
f	1078/1078	$C_{60}O_2(OOML)^-$
g	1095/1095	$C_{60}O_3(OOML)^-$
h	1111/1111	$C_{60}O_4(OOML)^-$

(b)

FIGURE 4: Mass spectra of the crude product on the reaction of  $C_{60}$  with an excess amount of methyl linoleate by heating under air.

radical of methyl linoleate (MLOO\*) was revealed to give fullerene multioxides ( $C_{60}O_n$ ) and their radical addition products [ $C_{60}(O)_n(OOML)_m$ ] along with their fragment peaks (Figures 3 and 4). This could be a part of evidence for a radical trap mechanism of fullerene  $C_{60}$ . On the other hand, no peaks derived from MLOO\* were obtained in the reaction of  $C_{60}(OH)_8$  with ML by mass and NMR spectroscopy. Although it failed to detect the product in this case, the disappearance of mass peaks corresponding to the starting  $C_{60}(OH)_8$ , which were observed before the reaction, implied that the fullerenol reacted with ML.

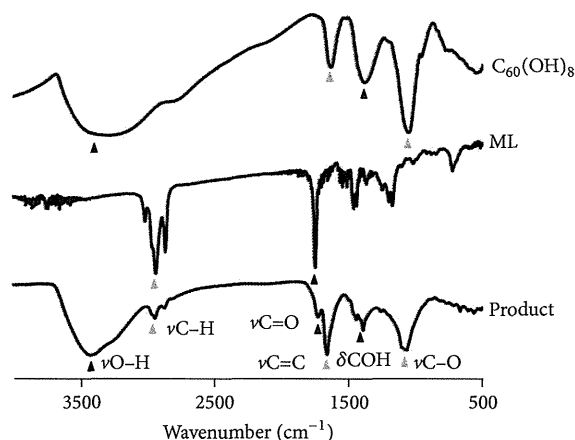


FIGURE 5: IR spectra of the crude product on the reaction of fullereneol  $C_{60}(OH)_8$  with methyl linoleate (ML) under autoxidation condition along with those of the starting materials.

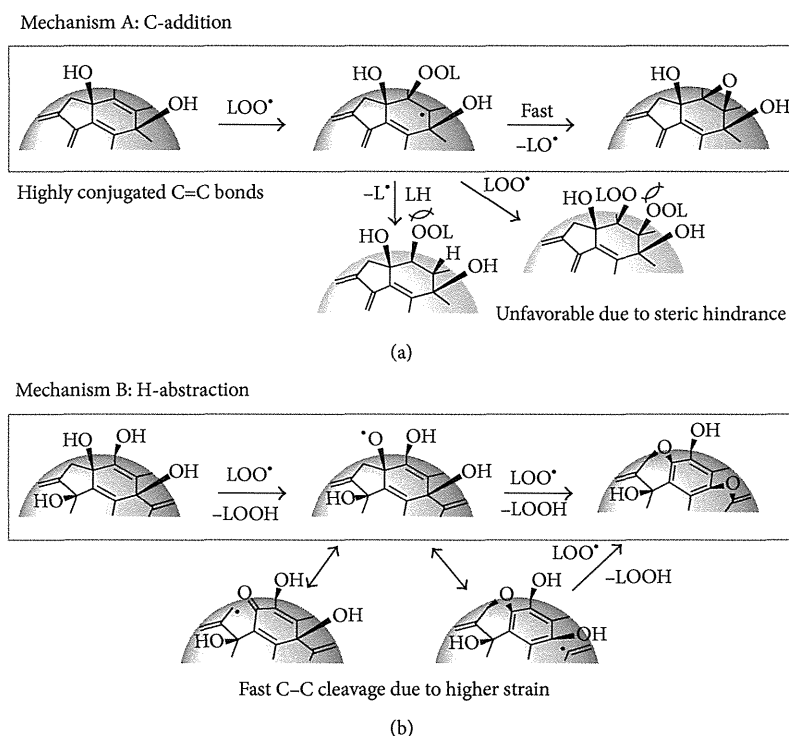


FIGURE 6: Possible mechanisms for lipid peroxyl radical ( $LOO^\bullet$ ) scavenging by fullereneols  $C_{60}(OH)_n$ : (a) addition to C=C double bonds for less hydroxylated fullerenes and (b) H-abstraction from -OH group for highly hydroxylated ones.

Instead of the failed mass analysis, the reaction product of fullereneol  $C_{60}(OH)_8$  with ML was analysed by IR spectroscopy (Figure 5). Even after reprecipitation of the product from diethyl ether/hexane = 9/1 followed by Florisil column chromatography with an eluent of THF, the small peak at ca.  $1700\text{ cm}^{-1}$  assigned for  $\nu C=O$  was observed along with the peaks at ca.  $2900\text{ cm}^{-1}$  assigned for  $\nu C-H$ . These signals may appear by the addition of  $MLOO^\bullet$  which has an ester moiety

or by the hydrogen abstraction from hydroxyl group with the subsequent carbonyl group formation (vide infra).

By considering the above results, we proposed two possible radical scavenging mechanisms of fullereneols as shown in Figure 6. One is "C-addition" type, which includes the peroxyl radical addition to a conjugated C=C double bond (mechanism A), and the other is "H-abstraction" type, which includes hydrogen atom abstraction from -OH group and the

subsequent skeletal rearrangement of fullereryl cage forming ether bridge (mechanism B). Lowly hydroxylated fullerlenols  $C_{60}(OH)_n$  ( $n = \text{ca. } 10$ ) which have enough  $\pi$ -conjugated double bonds probably favour the “C-addition” mechanism similar to the pristine  $C_{60}$ . By contrast, highly hydroxylated fullerlenols  $C_{60}(OH)_n$  ( $n = \text{ca. } 40$ ) seem to be relatively difficult to undergo the C-addition of  $MLOO^*$  because they have less and unreactive double bonds in addition to the larger steric hindrance from the crowded hydroxyl groups. The latter mechanism is the same as catechin (polyphenol) type and it is supported by the fact that some fullerlenols have acidic (similar to phenolic) hydroxyl groups. Because highly hydroxylated fullerlenols have larger strain on fullereryl cage due to the conversion of many  $sp^2$  carbons into  $sp^3$  carbons by hydroxylation, H-abstraction may be followed by the subsequent skeletal rearrangement on  $C_{60}$  cage to release the strain energy, forming some ether bridge. Fullerlenols  $C_{60}(OH)_n$  ( $n = \text{ca. } 24$ ) result in poor antioxidant activity probably due to the lack of both effects.

Finally, we also measured the antioxidant activity of several alcohols and phenols. Under the same condition of  $\beta$ -carotene bleaching assay, ethanol, *t*-butyl alcohol, benzyl alcohol, allyl alcohol, phenol, and *p*-bromophenol did not show antioxidant activity in spite of the existence of hydroxyl groups and unsaturated structures. The result clearly suggests the importance of high conjugation and distorted structure of fullerlenols for the antioxidant activity in  $\beta$ -carotene bleaching assay.

#### 4. Conclusions

In conclusion, we systematically evaluated the antioxidant activity of variously hydroxylated fullerlenols by  $\beta$ -carotene bleaching assay. The antioxidant activity %AOA was varied from 32% to 70% by changing the number of hydroxyl groups and both lowly hydroxylated  $C_{60}(OH)_{12}$  (70.1%) and highly hydroxylated  $C_{60}(OH)_{44}$  (66.0%) showed relatively high antioxidant activity. The obtained relative radical scavenging rate of fullerene  $k_{rel}$  toward radical species derived from linoleic acid under autoxidation condition indicated that these fullerlenols reacted 1.62 and 1.54 times faster than  $\beta$ -carotene, respectively. By the product analysis using the model reaction of  $C_{60}$  and methyl linoleate under autoxidation condition, we detected several mass peaks of radical scavenged fullerene derivatives as well as the IR spectra. These results suggest that the high  $\pi$ -conjugation and the strained structure of fullerlenol are responsible for the high radical scavenging reactivity and thus we proposed two possible antioxidant mechanisms, such as C-addition type and H-abstraction type, which are dependent on the number of hydroxyl groups.

#### Conflict of Interests

The authors declare that there is no conflict of interests regarding the publication of this paper.

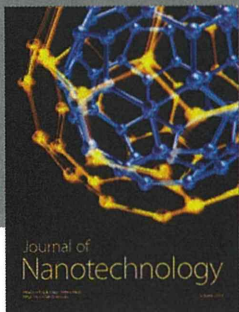
#### Acknowledgments

This work was supported by Health Labor Sciences Research Grants from MHLW, Japan. The authors thank Dr. H. Aoshima (Vitamin C60 BioResearch Corporation) for helpful discussion.

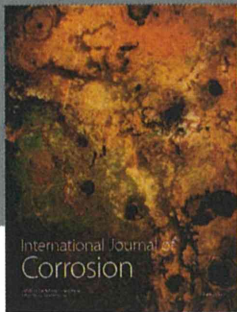
#### References

- [1] P. J. Krusic, E. Wasserman, P. N. Keizer, J. R. Morton, and K. F. Preston, “Radical reactions of  $C_{60}$ ,” *Science*, vol. 254, no. 5035, pp. 1183–1185, 1991.
- [2] H. Takada, K. Kokubo, K. Matsubayashi, and T. Oshima, “Antioxidant activity of supramolecular water-soluble fullerlenes evaluated by  $\beta$ -carotene bleaching assay,” *Bioscience, Biotechnology and Biochemistry*, vol. 70, no. 12, pp. 3088–3093, 2006.
- [3] K. Matsubayashi, T. Goto, K. Togaya, K. Kokubo, and T. Oshima, “Effects of pin-up oxygen on [60]fullerene for enhanced antioxidant activity,” *Nanoscale Research Letters*, vol. 3, no. 7, pp. 237–241, 2008.
- [4] L. Y. Chiang, F.-J. Lu, and J.-T. Lin, “Free radical scavenging activity of water-soluble fullerlenols,” *Journal of the Chemical Society, Chemical Communications*, no. 12, pp. 1283–1284, 1995.
- [5] S. Kato, H. Aoshima, Y. Saitoh, and N. Miwa, “Highly hydroxylated or  $\gamma$ -cyclodextrin-bicapped water-soluble derivative of fullerene: the antioxidant ability assessed by electron spin resonance method and  $\beta$ -carotene bleaching assay,” *Bioorganic and Medicinal Chemistry Letters*, vol. 19, no. 18, pp. 5293–5296, 2009.
- [6] Y. Saitoh, L. Xiao, H. Mizuno et al., “Novel polyhydroxylated fullerene suppresses intracellular oxidative stress together with repression of intracellular lipid accumulation during the differentiation of OP9 preadipocytes into adipocytes,” *Free Radical Research*, vol. 44, no. 9, pp. 1072–1081, 2010.
- [7] Y. Saitoh, A. Miyanishi, H. Mizuno et al., “Super-highly hydroxylated fullerene derivative protects human keratinocytes from UV-induced cell injuries together with the decreases in intracellular ROS generation and DNA damages,” *Journal of Photochemistry and Photobiology B*, vol. 102, no. 1, pp. 69–76, 2011.
- [8] Y. Saitoh, H. Mizuno, L. Xiao, S. Hyoudou, K. Kokubo, and N. Miwa, “Polyhydroxylated fullerene  $C_{60}(OH)_{44}$  suppresses intracellular lipid accumulation together with repression of intracellular superoxide anion radicals and subsequent PPAR $\gamma$ 2 expression during spontaneous differentiation of OP9 preadipocytes into adipocytes,” *Molecular and Cellular Biochemistry*, vol. 366, no. 1–2, pp. 191–200, 2012.
- [9] G. D. Nielsen, M. Roursgaard, K. A. Jensen, S. S. Poulsen, and S. T. Larsen, “In vivo biology and toxicology of fullerenes and their derivatives,” *Basic & Clinical Pharmacology & Toxicology*, vol. 103, no. 3, pp. 197–208, 2008.
- [10] J. Gao, Y. Wang, K. M. Folta et al., “Polyhydroxy fullerenes (fullerols or fullerlenols): beneficial effects on growth and lifespan in diverse biological models,” *PLoS ONE*, vol. 6, no. 5, Article ID e19976, 8 pages, 2011.
- [11] Z. Chen, L. Ma, Y. Liu, and C. Chen, “Applications of functionalized fullerenes in tumor theranostics,” *Theranostics*, vol. 2, no. 3, pp. 238–250, 2012.
- [12] K. Kokubo, S. Shirakawa, N. Kobayashi, H. Aoshima, and T. Oshima, “Facile and scalable synthesis of a highly hydroxylated water-soluble fullerlenol as a single nanoparticle,” *Nano Research*, vol. 4, no. 2, pp. 204–215, 2011.

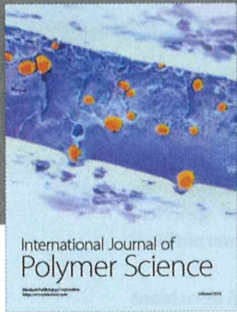
- [13] K. Kokubo, K. Matsubayashi, H. Tategaki, H. Takada, and T. Oshima, "Facile synthesis of highly water-soluble fullerenes more than half-covered by hydroxyl groups," *ACS Nano*, vol. 2, no. 2, pp. 327–333, 2008.
- [14] H. Ueno, K. Kokubo, E. Kwon, Y. Nakamura, N. Ikuma, and T. Oshima, "Synthesis of a new class of fullerene derivative  $\text{Li}^+@C_{60}O^-(\text{OH})_7$  as a "Cation-encapsulated anion nanoparticle";" *Nanoscale*, vol. 5, pp. 2317–2321, 2013.
- [15] G. Zhang, Y. Liu, D. Liang, L. Gan, and Y. Li, "Facile synthesis of isomerically pure fullerlenols and formation of spherical aggregates from  $C_{60}(\text{OH})_8$ ," *Angewandte Chemie International Edition*, vol. 49, pp. 5293–5295, 2010.
- [16] M. S. Al-Saikh, L. R. Howard, and J. C. Miller Jr., "Antioxidant activity and total phenolics in different genotypes of potato (*Solanum tuberosum*, L.)," *Journal of Food Science*, vol. 60, pp. 341–347, 1995.
- [17] A. Djordjevic, J. M. Canadanovic-Brunet, M. Vojinovic-Miloradov, and G. Bogdanovic, "Antioxidant properties and hypothetical radical mechanism of fullereneol  $C_{60}(\text{OH})_{24}$ ," *Oxidation Communications*, vol. 27, no. 4, pp. 806–812, 2004.
- [18] H. Aoshima, K. Togaya, T. Goto et al., "Evaluation of antioxidant activity of fullerenes and their inhibition effects on photodegradation of cosmetic ingredients," *Journal of Japanese Cosmetic Science Society*, vol. 33, pp. 149–154, 2009.
- [19] L. Y. Chiang, L.-Y. Wang, J. W. Swirczewski, S. Soled, and S. Cameron, "Efficient synthesis of polyhydroxylated fullerene derivatives via hydrolysis of polycyclosulfated precursors," *Journal of Organic Chemistry*, vol. 59, no. 14, pp. 3960–3968, 1994.
- [20] G. W. Burton and K. U. Ingold, " $\beta$ -Carotene: an unusual type of lipid antioxidant," *Science*, vol. 224, no. 4649, pp. 569–573, 1984.
- [21] K. Fukuzumi, N. Ikeda, and M. Egawa, "Phenothiazine derivatives as new antioxidants for the autoxidation of methyl linoleate and their reaction mechanisms," *Journal of the American Oil Chemists' Society*, vol. 53, no. 10, pp. 623–627, 1976.



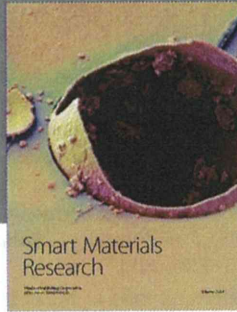
Journal of  
Nanotechnology



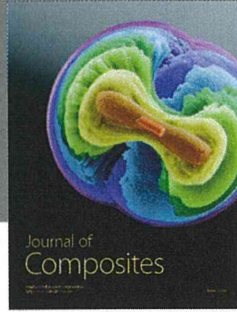
International Journal of  
Corrosion



International Journal of  
Polymer Science




Smart Materials  
Research



Journal of  
Composites

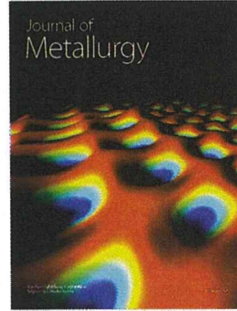


BioMed  
Research International

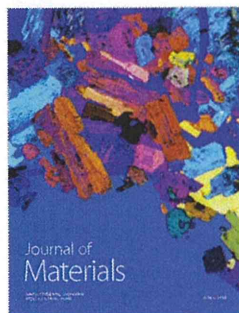


**Hindawi**

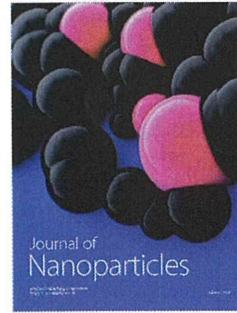
Submit your manuscripts at  
<http://www.hindawi.com>



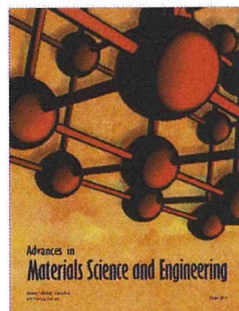
Journal of  
Metallurgy



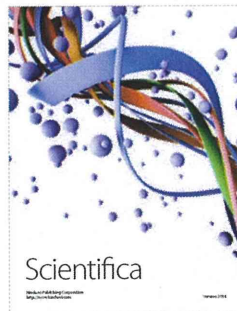
Journal of  
Materials



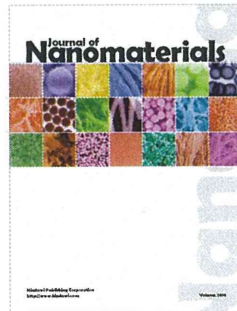
Journal of  
Nanoparticles



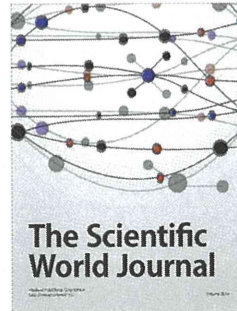
Advances in  
Materials Science and Engineering



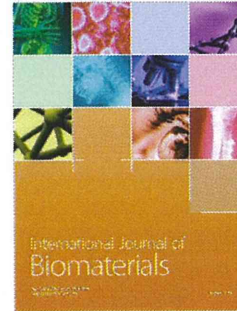
Scientifica



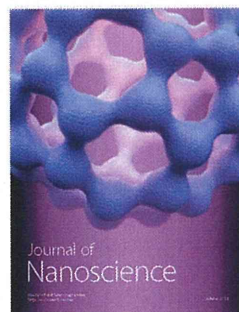
Journal of  
Nanomaterials



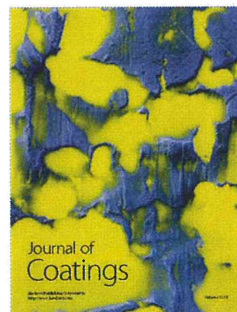
The Scientific  
World Journal



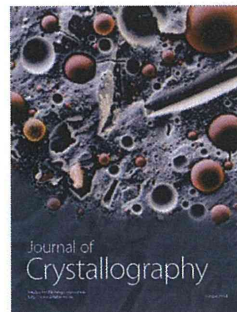
International Journal of  
Biomaterials



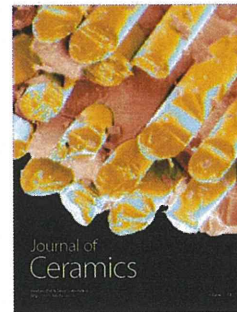
Journal of  
Nanoscience



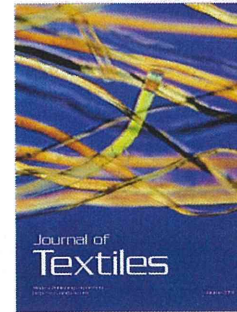
Journal of  
Coatings



Journal of  
Crystallography



Journal of  
Ceramics



Journal of  
Textiles

HETEROCYCLES, Vol. 90, No. 2, 2015, pp. 1168 - 1178. © 2015 The Japan Institute of Heterocyclic Chemistry  
Received, 28th July, 2014, Accepted, 28th August, 2014, Published online, 11th September, 2014  
DOI: 10.3987/COM-14-S(K)92

## SYNTHESIS OF PYRROLIDINOFULLERENES VIA SINGLE ELECTRON TRANSFER REACTION OF ARYLDIENAMINES WITH C<sub>60</sub>

Naohiko Ikuma,\* Hiroyuki Yamamoto, Ken Kokubo, Takumi Oshima

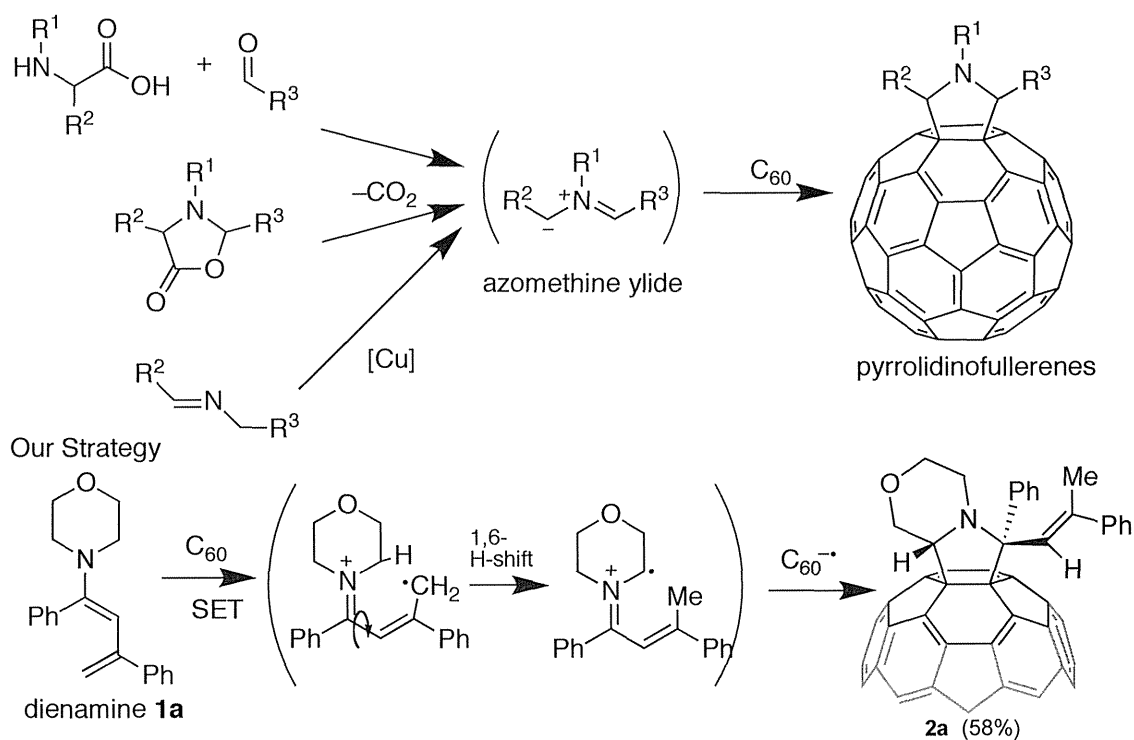
Division of Applied Chemistry, Graduate School of Engineering, Osaka University, Osaka 565-0871, Japan

E-mail: ikuma@chem.eng.osaka-u.ac.jp

**Abstract** – Various aryl-substituted pyrrolidinofullerenes were synthesized via a single electron transfer (SET) reaction of diaryldienamines with C<sub>60</sub> and the following consecutive 1,6-hydrogen shift and the [3 + 2] cycloaddition of the generated radical ion pair. The LUMO levels of pyrrolidinofullerenes were ca. 0.1 eV higher than C<sub>60</sub>, consequently suppressing the bisadduct formation. The phenyl-substituted pyrrolidinofullerene **2a** representatively exhibited the protic acid-catalyzed intramolecular Friedel–Crafts cyclization and the DDQ induced oxidative reversion into C<sub>60</sub>.

### INTRODUCTION

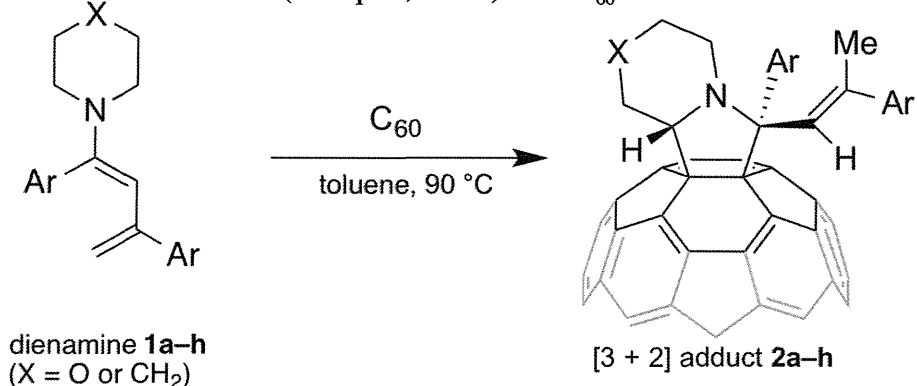
Pyrrolidinofullerenes<sup>1–6</sup> are useful fullerene derivatives in materials chemistry and for medicinal applications, as liquid crystals,<sup>5</sup> light-converting substances,<sup>6</sup> and chiral fullerene compounds.<sup>3,4</sup> These fullerenes are easily synthesized from the [3 + 2] cycloaddition of azomethine ylides which were prepared from various precursors such as carbonyl compound/amino acid (Prato reaction),<sup>1,2</sup> aziridine,<sup>1,3</sup> lactone,<sup>1</sup> and imine.<sup>4</sup> In very recent communication, we have reported that morpholinodiphenyldienamine **1a** underwent a single electron transfer (SET) reaction with C<sub>60</sub> to give diarylpyrrolidinofullerene **2a** via the subsequent 1,6-hydrogen shift and the [3 + 2] cycloaddition of the radical cation with C<sub>60</sub> radical anion (Scheme 1).<sup>7</sup> We also confirmed the reaction mechanism by DFT calculations as well as the radical-trapping experiment. In this paper, we report the synthesis of variously aryl-substituted pyrrolidinofullerenes by way of this SET/H-shift process. Moreover, we have examined the electronic properties and thermal stability (by DSC and TGA), TfOH catalyzed transformation, and DDQ induced oxidative degradation.



Scheme 1

## RESULTS AND DISCUSSION

As in the case of **2a**, variously aryl-substituted pyrrolidinofullerenes **2b–h** were synthesized as shown in Table 1. Dienamines **1b–h** were prepared by the condensation of arylketones and cyclic amines with *p*-toluenesulfonic acid (TsOH) catalyst. Due to the lability, less volatile dienamines **1b–h** were immediately used for the reaction with  $C_{60}$  without further purification and identification. These crude dienamines (ca. 25 equiv) were reacted with  $C_{60}$  in toluene at 90 °C. The reaction was traced by HPLC (Buckyprep column, toluene eluent). Unfavorable contaminants such as enamines and unreacted arylketones appreciably neither inhibited the present cycloaddition nor brought about the side reactions. The reaction solution was evaporated and the residue was submitted for column chromatography to give pure monoadducts **2b–h** in slightly lower yields (ca. 20–40 %) than **2a**. Piperidinodienamine **1b** reacted faster than morpholinodienamine **1a** on account of higher electron-donating piperidine substituent, so that the isolated yield of **2b** slightly decreased due to the formation of multiadducts. Similarly, the reaction of morpholinodienamines with donative aryl groups such as 4-alkylphenyl (**1d–f**) and thiophene **1h** gave slightly lower yields because of the multiaddition. On the other hand, *p*-chlorophenyl-substituted dienamine **1c** needed slightly longer reaction time because of lower electron-donating ability. The  $^1\text{H}/^{13}\text{C}$  NMR spectra of these 1:1 adducts showed similar signals to those of **2a**; appearances of methyl group and asymmetric morpholino/piperidino ring were only explained by the hydrogen shift of dienamino radical cation and [3 + 2] cycloaddition.

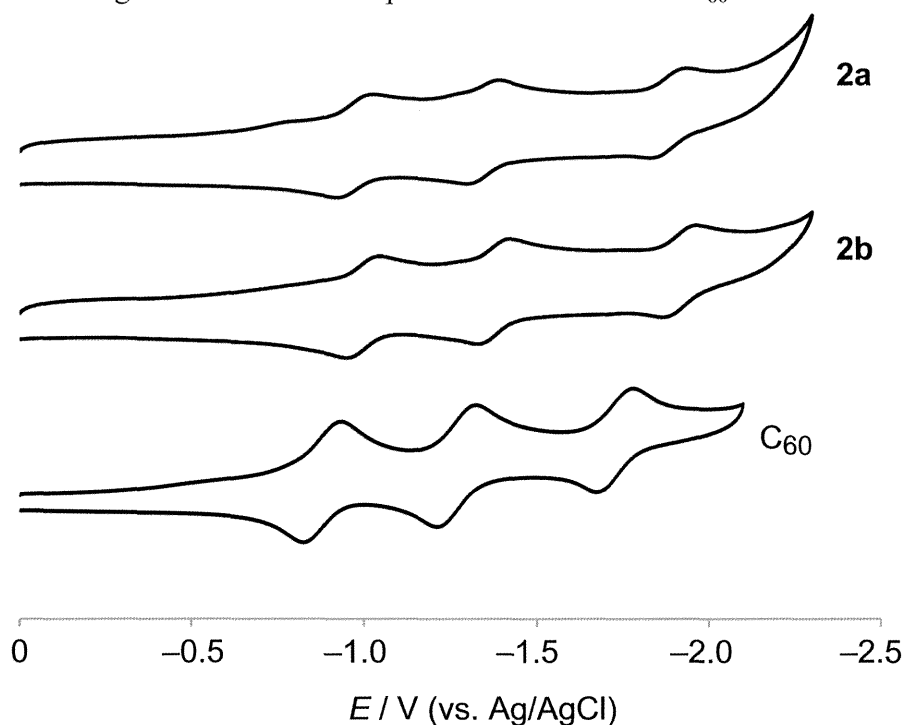
**Table 1.** Reaction of dienamines **1a–h** (25 equiv, 90 °C) with C<sub>60</sub>

	Amine	Ar	Time (h)	Conv. (%) <sup>b</sup>	Yield (%) <sup>c</sup>
<b>1a<sup>a</sup></b>			17	89	58
<b>1b</b>			3.5	92	33
<b>1c</b>			20	87	42
<b>1d</b>			14	88	30
<b>1e</b>			15	88	29
<b>1f</b>			16	90	24
<b>1g</b>			16	90	42
<b>1h</b>			17	83	21

<sup>a</sup>From the preliminary communication.<sup>7</sup> <sup>b</sup>Determined by HPLC area ratio. <sup>c</sup>Isolated yields.

For the application to electronic materials, we estimated the electron affinity of pyrrolidinofullerenes **2a–h**. Cyclic voltammogram measurements showed ca. 0.1 V lower reduction potentials than that of C<sub>60</sub>, implying the pyrrolidino-fusion lowered the electrophilicity of fullerene core (Table 2). This lowering electron affinity of monoadducts will suppress further SET reaction giving bisadducts. However, these substituent effects are not so effective because of indirect inductive effect of the aryl substituents.



**Table 2.** Cyclic voltammograms and reduction potentials of **2a–h** and C<sub>60</sub> in *o*-DCB<sup>a</sup>

Compd	$E^{1/2}$ V vs Fc/Fc <sup>+</sup>		
	$E_{1\text{red}}$ (LUMO level/eV) <sup>b</sup>	$E_{2\text{red}}$	$E_{3\text{red}}$
<b>2a</b>	-1.17 (-3.63)	-1.55	-2.08
<b>2b</b>	-1.20 (-3.60)	-1.58	-2.12
<b>2c</b>	-1.16 (-3.64)	-1.54	-2.07
<b>2d</b>	-1.18 (-3.62)	-1.56	-2.10
<b>2e</b>	-1.14 (-3.66)	-1.53	-2.06
<b>2f</b>	-1.15 (-3.65)	-1.53	-2.08
<b>2g</b>	-1.15 (-3.65)	-1.55	-2.11
<b>2h</b>	-1.16 (-3.64)	-1.55	-2.09
C <sub>60</sub>	-1.08 (-3.72)	-1.46	-1.91

<sup>a</sup>Electrolyte 0.1 M TBAP; scan rate 100 mV s<sup>-1</sup>; potentials measured vs Ag/Ag<sup>+</sup> reference electrode and standardized to Fc/Fc<sup>+</sup> couple [ $E_{\text{Fc/Fc}^+} = +0.203$  V vs Ag/Ag<sup>+</sup> (*o*-DCB)]. <sup>b</sup>Values from the vacuum level were estimated using the following equation; LUMO level =  $-(E_{1\text{red}}^{1/2} + 4.8)$ .<sup>8</sup>

Thermal stability of **2a** was evaluated by DSC (Figure 1a) and TGA (Figure 1b) measurements. One endothermic peak followed by exothermic plateau in DSC and drastic weight loss (ca. 13%) in TGA were observed around 260–270 °C, suggesting melting with decomposition. This decomposition temperature is comparable with those of pyrrolidinofullerenes bearing BOC-group (>250 °C),<sup>6b</sup> but lower than those of liquid pyrrolidinofullerenes with stable alkoxyphenyl groups (340–420 °C).<sup>9</sup> These previous studies indicate the pyrrolidino ring seems to be stable around 300 °C unless the compound has less stable substituents such as BOC group. Thus we can consider the decomposition of **2a** at 265 °C is due to the

elimination of methylstyrene moiety, in consistent with the weight loss of TGA (F.W. of CH=CMePh is 117, whereas M.W. of **2a** is 1012).<sup>10</sup>

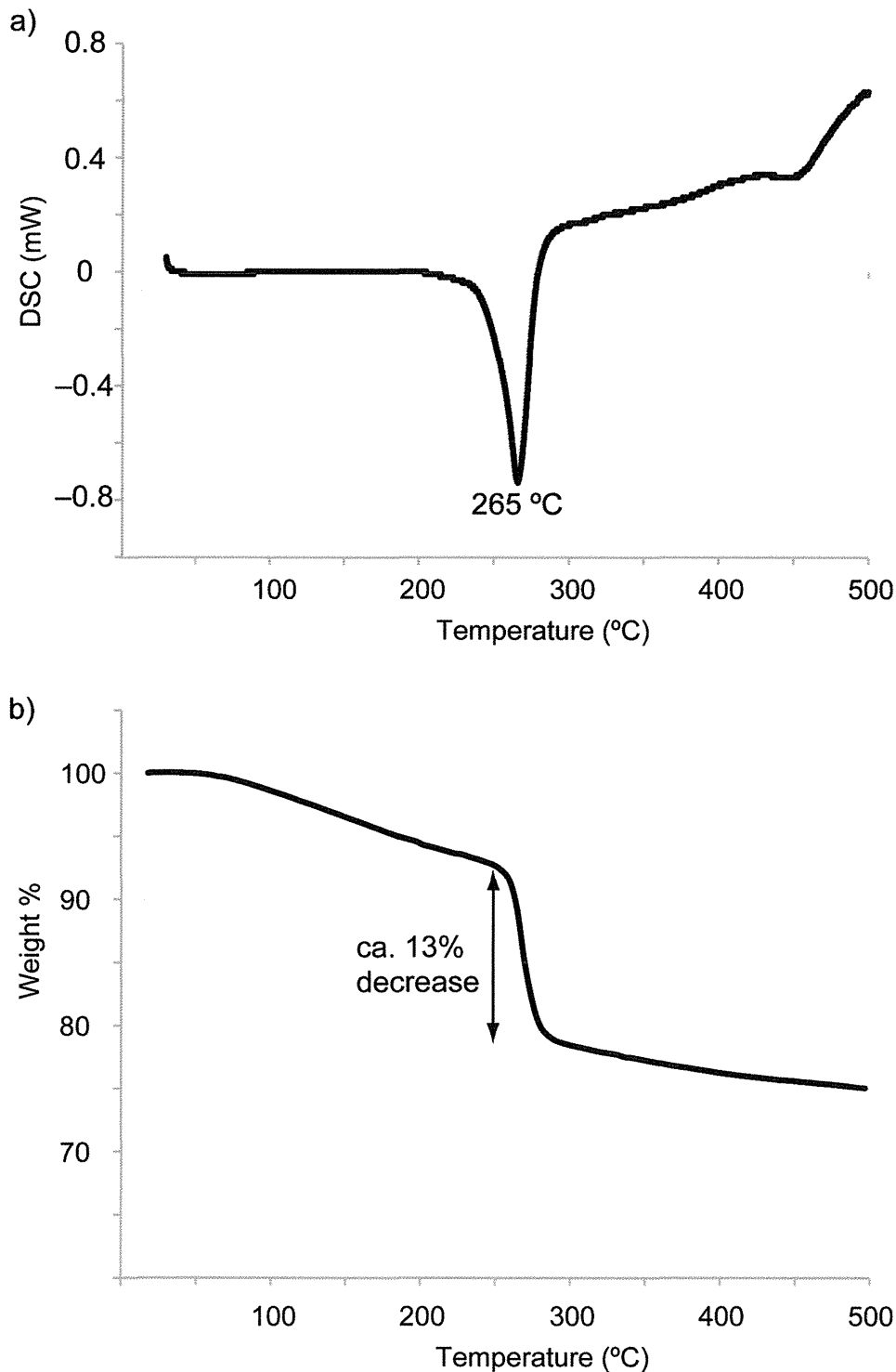
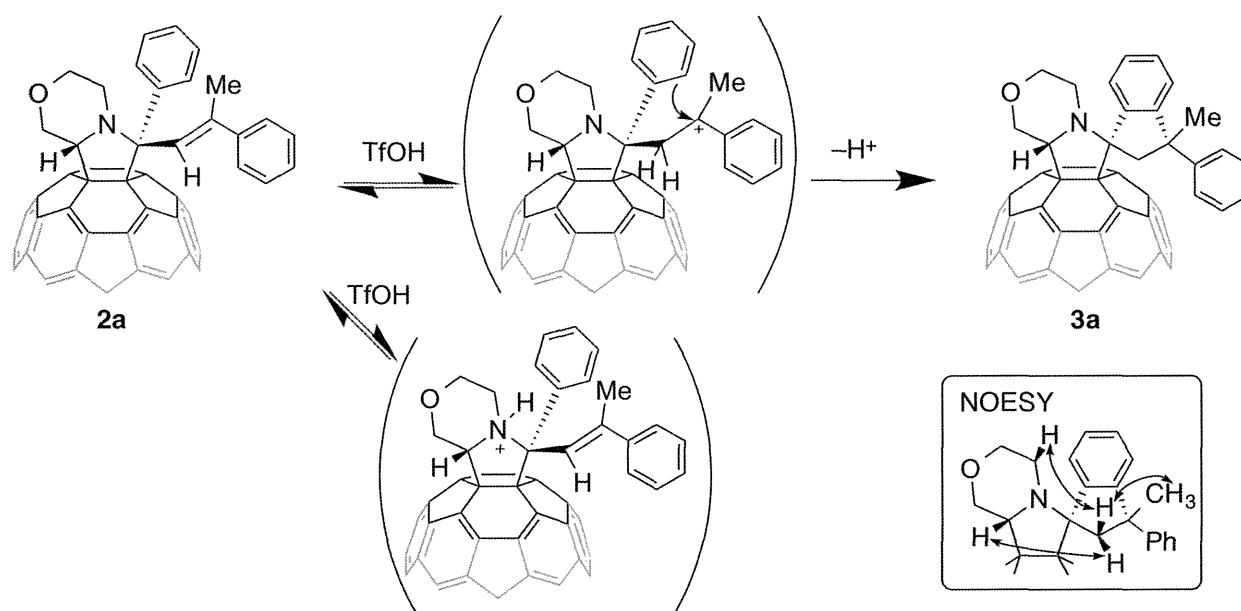


**Figure 2.** a) DSC and b) TGA measurements of **2a** under N<sub>2</sub> atmosphere.

We have carried out acid treatment of **2a** because these pyrrolidinofullerenes inherently have basic site at the nitrogen of pyrrolidino moiety. However, by adding excess amount of TfOH (25 equiv), the amino linkage was retained but the intramolecular Friedel–Crafts type cyclization occurred to give spiro

compound **3a** (Scheme 2) as confirmed by  $^1\text{H}/^{13}\text{C}$  NMR and 2D-HSQC/HMBC/NOESY correlation (Supporting Information). Similar to styrene which easily polymerizes with electrophilic initiator, phenylvinyl group of **2a** may be protonated at the  $\beta$ -position to form relatively stable benzylic carbocation. This cationic center is attacked by adjoining phenyl ring to construct the stable dihydroindene ring.<sup>11</sup> In this acid treatment, although pyrrolidino function can be protonated, the resulting quarterly ammonium ion seems to persist any further transformation. The reaction proceeded in various polar aromatic solvents such as *o*-DCB, and anisole (Table 3). Anisole and toluene provided slightly lower yield, probably because these solvents are likely to participate in the Friedel–Crafts reaction at the fullerene sphere.<sup>12,13</sup>



Scheme 2

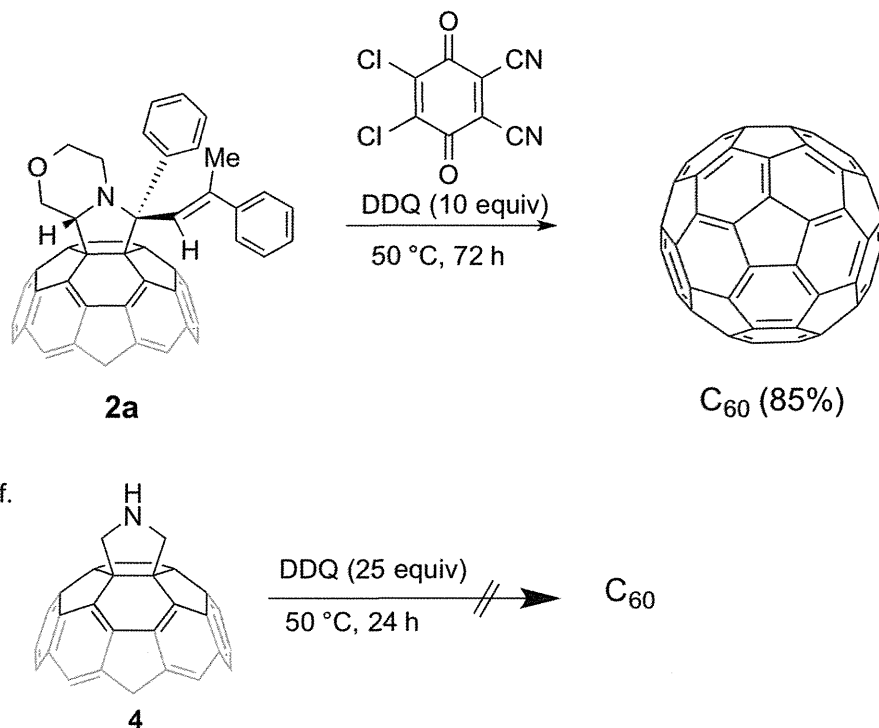
Table 3. Reaction of **2a** with TfOH (25 equiv) in various solvents

Solvent	Temp (°C)	Time (h)	Conversion (%) <sup>a</sup>	Yield of <b>3a</b> (%) <sup>b</sup>
benzene	80	3	98	40
toluene	80	4	95	27
chlorobenzene	80	5	95	59
anisole	80	5	90	28
<i>o</i> -DCB	80	5	90	56
DMF	80	24	-	-
chloroform	80	24	20	5

<sup>a</sup> Determined by HPLC area ratio. <sup>b</sup> Isolated yields.

Pyrrolidinofullerenes are known to undergo the cycloreversion into azomethine ylide and  $\text{C}_{60}$  under the influence of oxidant such as Cu(II) and trapping dipolarophiles.<sup>14</sup> Similarly, oxidation of **2a** by DDQ led to the regeneration of  $\text{C}_{60}$  even without trapping agents (Scheme 3). Since the unsubstituted

pyrrolidinofullerene **4**<sup>1</sup> was not oxidized by DDQ, the oxidative abstraction of methine proton of pyrrolidine ring of **2a** seems to be essential for the cycloreversion.



Scheme 3

## EXPERIMENTAL

**General Synthetic Procedure of 2:** The solution of cyclic amines (100 mmol), arylketone (100 mmol), and catalytic amount of *p*-toluenesulfonic acid (TsOH, <100 mg) in toluene (50 mL) was stirred at refluxing temperature (140 °C) under nitrogen for 5–10 h using a Dean-Stark apparatus. After the removal of solvent, unreacted acetophenone and morpholine were almost removed in vacuo. The residue was diluted with pentane to precipitate TsOH, then filtrated and evaporated. Crude products **1b–h** were employed in the next reaction without further purifications. The solution of C<sub>60</sub> (100 mg, 0.14 mmol) and dienamines **1** (ca. 3.5 mmol, 25 equiv) in toluene (50 mL) was stirred in dark at 90 °C under nitrogen. The reaction was traced by HPLC (Buckyprep, toluene eluent). After filtration, the solvent was removed in vacuo. The residue was chromatographed on silica gel to provide the monoadduct **2b–h**.

**Compound 2b.** <sup>1</sup>H-NMR: (600 MHz, CDCl<sub>3</sub>) δ 1.80 (s, 3H), 2.01–2.09 (m, 2H), 2.17–2.23 (m, 2H), 2.31–2.34 (dd, 1H, *J* = 6.8, 13.4 Hz), 2.71–2.74 (m, 2H), 3.61–3.63 (d, 1H, *J* = 10.9 Hz), 4.59–4.61 (dd, 1H, *J* = 3.0, 11.2 Hz), 7.25–7.27 (m, 2H), 7.30–7.33 (t, 1H, *J* = 7.5 Hz), 7.38–7.41 (t, 2H, *J* = 7.9 Hz), 7.45–7.48 (m, 1H), 7.46 (s, 1H), 7.59–7.61 (d, 2H, *J* = 7.3 Hz), 7.71–7.73 (d, 1H, *J* = 6.9 Hz), 8.23–8.24 (d, 1H, *J* = 8.0 Hz). <sup>13</sup>C-NMR: (150 MHz, CDCl<sub>3</sub>) δ 20.73, 25.26, 25.88, 32.33, 47.77, 69.99, 73.41, 79.71, 81.97, 126.39, 127.41, 127.72, 127.75, 127.80, 128.25, 128.69, 128.86, 130.28, 135.81, 136.03, 136.53, 137.49, 138.51, 139.42, 139.49, 139.96, 140.25, 141.24, 141.60, 141.65, 141.75, 141.78, 141.93,